Centroid shifts of spatiotemporal vortex pulses with arbitrarily oriented orbital angular momentum at planar reflection and refraction

Fangqing Tang and Lixiang Chen*
Department of Physics, Xiamen University, Xiamen 361005, China

(Received 10 December 2023; accepted 12 February 2024; published 11 March 2024)

The vortex structure of wave packets on the transversal or spatiotemporal plane can significantly enhance their shifts during the reflection and refraction. These shifts are classified into six types: Goos-Hänchen shift within the plane of incidence, Imbert-Fedorov shift perpendicular to the plane of incidence, longitudinal shift, together with three counterparts of angular shifts. Here, we analytically derive the expressions for these shifts for three-dimensional spatiotemporal vortex wave packets that carry orbital angular momentum of arbitrary orientation. It is found that the influence of the optical configurations (e.g., incident angle, refractive index, etc.) on the shifts can be described by a deformation tensor, while that of the wave-packet structure is an isotropic one. Interestingly, the spatial and angular shifts induced by the topological charge can be attributed to two topologically distinct tangent vector fields on the spheres, respectively. Also, the conservation laws of transverse linear momentum and vertical angular momentum are revisited. Our studies may find potential in spatiotemporal pulse shaping and shed light on the recent controversy regarding the definition of intrinsic orbital angular momentum for a spatiotemporal vortex pulse.

DOI: 10.1103/PhysRevA.109.033512

I. INTRODUCTION

The problem of plane-wave refraction and reflection on planar interfaces can be resolved using Snell's law and the Fresnel equations [1]. Pertaining to a realistic light pulse, such as a Gaussian wave packet, it exhibits a finite frequency and spatial broadening along its central wave vector. The superposition of infinite plane waves can cause the spatial centroid of the reflected and transmitted pulses to deviate from the origin. These shifts include the Goos-Hänchen (GH) shift within the incident plane, perpendicular to the propagation direction, which is associated with the spatial gradient of the Fresnel coefficients [2,3]. While the shift along the propagation direction caused by the frequency dependence of Fresnel coefficients can lead to a longitudinal shift or temporal delay, known as the Wigner time delay [4,5]. The shift perpendicular to the incident plane is termed as the Imbert-Fedorov (IF) shift [6,7], with the most notable characteristic being its dependency on the handedness of the light's circular polarization state, which consequently leads to the spin Hall effect of light [8–11]. These shifts are on the same order of the wavelength and is related to its polarization state. Similarly, during the reflection and refraction processes, angular shifts or momentum shifts also occur probably, analogous to the aforementioned types [12–14]. These shifts are of the same order of the inverse of the Rayleigh length. Intriguingly, for higher-order vortex beams, these shifts are proportional to the topological charge [15–18].

Previous research has predominantly concentrated on the monochromatic vortex-structured beams with the orbital angular momentum (OAM) along the propagation direction, but rarely care about spatiotemporal coupled vortices, mainly because that it is not a long time after the experimental discoveries and manipulations of these spatiotemporal vortex wave packets (STVPs) [19–21]. These pulses, carrying OAM perpendicular to the propagation direction, provide a novel degree of freedom for photon manipulation, thereby holding substantial research value. Notably, Mazanov and Bliokh *et al.* recently reported their studies about the shifts of the STVPs in planar reflection and refraction, using a methodology akin to the analysis of monochromatic vortices to calculate these shifts [22]. They focused on two specific wave packets—type A and type B—with the vortex axes perpendicular to the propagation direction and a two-dimensionally broadened envelope. In general, the spatiotemporal coupled vortices can be arbitrarily oriented in space and can be prepared using various devices such as customized photonic crystal [23], astigmatic mode converter [24], tight-focusing lens based on spin-orbit coupling [25], a 4Pi optical configuration or a spatial chirp [26,27]. It just forms the incentive of our present work to provide a theoretical study for these shifts of a three-dimensionally polarized STVPs with an arbitrary spatially oriented OAM on planar reflection and refraction. First, we analytically derive the expressions of these shifts at the second-order correction approximation of wave vectors. We also verify the reliability of analytic solutions by comparing with precise numerical results. Second, by distinguishing the influences of configuration and the wave packet intrinsic structure, we reveal the mechanism of the influence of the orientation of OAM on these pulse shifts. This unified description establishes a connection between traditional monochromatic vortices and STVPs. Finally, we also examine the conservation laws involving transverse momentum and angular momentum (AM).

*chenlx@xmu.edu.cn

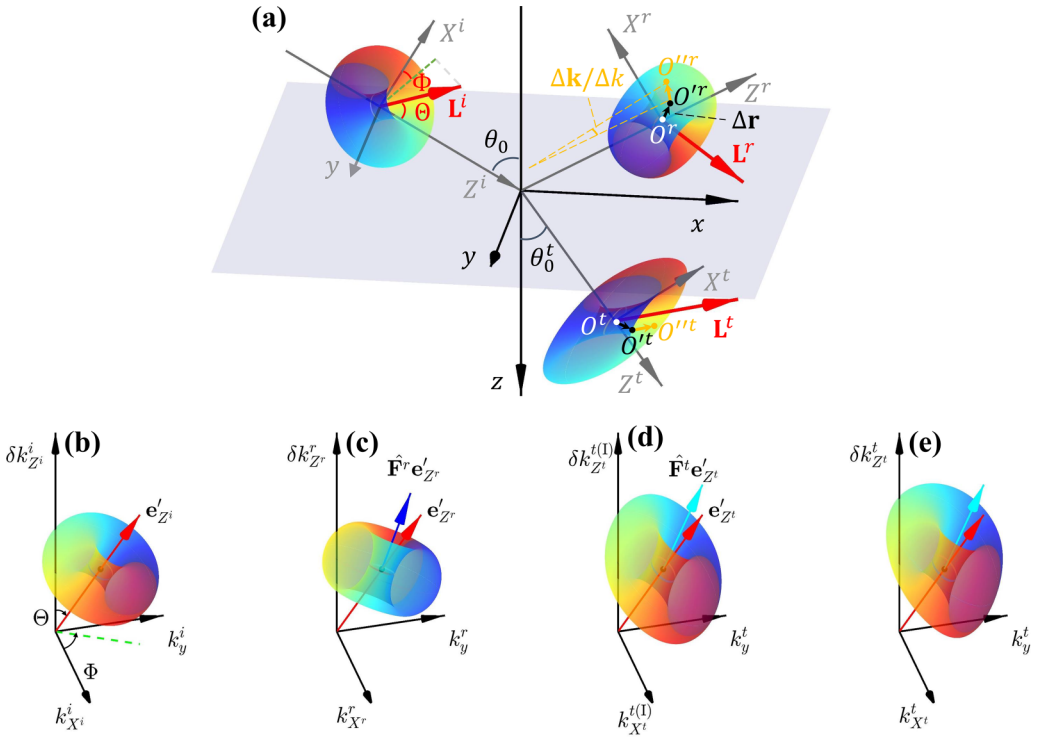

FIG. 1. The schematic diagram of reflection and refraction of a tilted STVPs at a planar interface is shown in panel (a). we use red, cyan, and blue arrows to denote the orientation of vortex lines of the pulse at incidence, reflection, and refraction, respectively. Their OAM directions are also denoted by red arrows. Shifts of centroid of the pulse include spatial shifts ($O^a \to O'^a$) and angular shifts ($O'^a \to O''^a$). Isointensity surfaces in the wave-vector space for the tilted STVPs at different stages: (b) incidence, (c) reflection, (d) refraction under the first-order wave-vector approximation, and (e) refraction under the second-order wave-vector approximation.

II. ANALYTICAL EXPRESSIONS FOR THE SHIFTS OF TILTED SPATIOTEMPORAL VORTEX WAVE PACKETS

As shown in Fig. 1, we consider an incident STVP with the vortex line along an arbitrary direction characterized by the azimuth Θ and the elevation Φ relative to the accompanying coordinate frame (X^i, y, Z^i) for the incident pulse. Similarly, the accompanying coordinate frames for the reflection and refraction are denoted (X^r, y, Z^r) and (X^t, y, Z^t), respectively. We use the superscript $a = i, r, t$ to represent incidence, reflection, and refraction, respectively. According to Snell's law, the STVP incident along the Z^i axis with an incidence angle θ_0 defines a refraction angle $\theta_0^t = \arcsin(n_0^{-1} \sin\theta_0)$, where n_0 is the refractive index.

The three-dimensional (3D) field of the incident pulse of a longitudinal vortex line (i.e., $\Theta = 0$) can be described by the Laguerre-Gaussian (LG) function with radial index zero and topological charge l,

$$\tilde{\mathbf{E}}^i(u, v, w) = \tilde{N}_l[u + i\mathrm{sgn}(l)v]^{|l|} e^{-\frac{(u^2+v^2+w^2)k_0^2 w_0^2}{4}} \tilde{\mathbf{e}}, \quad (1)$$

where $u = k_{X^i}/k_0$, $v = k_y/k_0$, and $w = (k_{Z^i} - k_0)/k_0$ are the relative deviations from the central wave vector along X^i, y, and Z^i, respectively. k_0 is the central wave number, w_0 is the spatial waist. $\tilde{N}_l$ is the normalized factor and $\tilde{\mathbf{e}} = e^{X^i}\mathbf{e}_{X^i} + e^y\mathbf{e}_y$ is the normalized Jones vector of uniformly distributed polarization of the field in the transverse plane, where we use the superscripts X^i or y to denote its corresponding component. Although Eq. (1) only gives the spatial envelope of the pulse, it also determines the temporal envelope according to the dispersion relation. For example, in free space, the longitudinal spatial waist w_0 also determines that the pulse duration equals w_0/c. Hereafter, we conduct our analysis within the three-dimensional spatial domain and will not repeat the temporal aspect. The pulse in free space carries intrinsic OAM with a value of $l/\omega\mathbf{e}_{Z^i}$ per unit intensity, where $\mathbf{e}_{Z^i}$ is the unit vector along Z^i. In general, the field of the STVP with titled angle (Θ, Φ) can be described by

$$\tilde{\mathbf{E}}^i(u, v, w) = \tilde{N}_l[u' + i\mathrm{sgn}(l)v']^{|l|} \times \exp\left[-\tfrac{1}{4}(u'^2 + v'^2 + w'^2)k_0^2 w_0^2\right]\tilde{\mathbf{e}}. \quad (2)$$

Here we introduce new parameters (u', v', w'), which are connected with the original parameters (u, v, w) by $(u', v', w')^T = R(\Theta, \Phi)(u, v, w)^T$. The related rotation matrix is

$$R(\Theta, \Phi) = \begin{pmatrix} \cos\Theta\cos\Phi & \cos\Theta\sin\Phi & -\sin\Theta \\ -\sin\Phi & \cos\Phi & 0 \\ \sin\Theta\cos\Phi & \sin\Theta\sin\Phi & \cos\Theta \end{pmatrix}. \quad (3)$$

It should be noted that the orientation of vortex line in space is the same as that in wave-vector space. The intrinsic OAM of this titled STVP becomes $l\mathbf{e}_n/\omega$, where $\mathbf{e}_n = (\sin\Theta\cos\Phi, \sin\Theta\cos\Phi, \cos\Theta)^T$ is the unit vector of the vortex line. The isointensity surface of the field in wave-vector space at incident and reflection or refraction are displayed in Figs. 1(b)–1(e).

For the pulse with finite size, the refracted wave vectors around the central wave undergo inhomogeneous

recombination based on Snell's law, and the reflected wave vectors experience a sign reversal along the X^a axis. In the paraxial and quasimonochromatic approximation, the first-order connection of the three components of the wave vectors between the refraction and reflection pulse and incidence pulse can be written as [18,22]

$$k_{X^a}^{a(\mathrm{I})} = k_0 \gamma^a u, \tag{4a}$$

$$k_y^{a(\mathrm{I})} = k_0 v, \tag{4b}$$

$$k_{Z^a}^{a(\mathrm{I})} = k_0 n_0^a (w+1), \tag{4c}$$

where $\gamma^r = -1$, $\gamma^t = \cos\theta_0/\cos\theta_0^t$, $n_0^r = 1$, and $n_0^t = n_0$. Hereafter, we refer these shifts as the first-order terms of the wave vector. For the longitudinal wave vector given in Eq. (4c), what we care about is the deviation from the central wave vector $\delta k_{Z^a}^a = k_{Z^a}^a - n_0^a k_0$. Here, we also analytically derived the second-order approximation of Snell's law (see Appendix A), where the second-order terms for the refraction wave vectors can be written as

$$k_{X^t}^{t(\mathrm{II})} = -\frac{k_0 \tan\theta_0^t \left(n_0^2-1\right)}{2n_0}\left(\frac{u^2}{\cos^2\theta_0^t}+v^2\right), \tag{5a}$$

$$k_{Z^t}^{t(\mathrm{II})} = \frac{k_0 \left(n_0^2-1\right)}{2n_0}\left(\frac{u^2}{\cos^2\theta_0^t}+v^2\right). \tag{5b}$$

In the derivation, we have also assumed that the medium's chromatic dispersion is sufficiently small to be ignored. The final calculated shifts thereby do not include the Wigner delay, Our subsequent derivations are also based on this approximation.

For a given field in the wave-vector space, the angular (or momentum) and spatial shifts can be obtained by calculating the expectation values of the wave vectors and spatial operators. The physical meaning of spatial shift is the deviation of the pulse's energy centroid relative to the pulse's center (the origin of the accompanying frame that moves with the pulse at the group velocity). Angular shift is the deviation of the average wave vector relative to the central wave vector, which can be transformed into the spatial shift during the propagation of the pulse (see Appendix B), as also shown in Fig. 1(a). The spatial or angular shifts are uniformly described by Eq. (B9) in Appendix B. We calculate these shifts at the moment $t = 0$ when the incident pulse just reaches the interface.

Next we describe the overall approach to solving this problem: Since the amplitude of the refracted and reflected pulse can only be determined using Fresnel's formula, we must calculate them under the wave-vector representation, where the position X^a becomes the operator form $\hat{X}^a = i\nabla^a$. We can replace the parameters from the refracted (reflected) wave vectors to the incident wave vector, then the position (wave vector) of the refraction (reflection) becomes a function of the incident wave vector. These functions have been calculated in Appendix A, and the functions describing the fields are also given in Appendix B. Eventually, Eq. (B9) is then written as an integral that depends explicitly on the parameters (u, v, w). For example, the shift of variable O^a in the refraction or reflection can be calculated as

$$\langle O^a \rangle^a = \frac{\iiint_{-\infty}^{+\infty} [\tilde{\mathbf{E}}^a(u,v,w)]^\dagger \hat{O}^a \tilde{\mathbf{E}}^a(u,v,w) du dv dw}{\iiint_{-\infty}^{+\infty} |\tilde{\mathbf{E}}^a(u,v,w)|^2 du dv dw}, \tag{6}$$

where $\hat{O}^a$ is the operator for this variable, $\tilde{\mathbf{E}}^a(u,v,w)$ is the field of the refraction or reflection and can be obtained by applying Fresnel's formula to the incident field. Note that the Fresnel coefficient matrix generally depends on the direction of wave vectors and frequencies. In the paraxial and quasimonochromatic approximation, we only need to consider their first-order terms relative to u, v, w, which is referred to as the effective Jones matrix and has been calculated in Ref. [18], see also Eq. (B7) in Appendix B. They can also be used in our case when the chromatic dispersion (or the difference between group velocity and phase velocity) can be ignored.

Meanwhile, in the first-order approximation of the wave vectors associated with the relative deviation from the central wave vector, the spatial operators can be described by

$$\hat{X}_a^{(\mathrm{I})} = i\frac{1}{k_0\gamma^a}\frac{\partial}{\partial u}, \tag{7a}$$

$$\hat{y}_a^{(\mathrm{I})} = i\frac{1}{k_0}\frac{\partial}{\partial v}, \tag{7b}$$

$$\hat{Z}_a^{(\mathrm{I})} = i\frac{1}{k_0 n^a}\frac{\partial}{\partial w}. \tag{7c}$$

We have also derived the expressions of spatial operators under the second-order approximation (see Appendix A), and the second-order terms are

$$\hat{X}_t^{(\mathrm{II})} = -i\frac{\left(n_0^2-1\right)}{k_0\gamma^t n_0^2\cos^2\theta_0} u\frac{\partial}{\partial w}, \tag{8a}$$

$$\hat{y}_t^{(\mathrm{II})} = i\frac{\tan\theta_0\left(n_0^2-1\right)}{k_0 n_0^2} v\frac{\partial}{\partial u} - i\frac{\left(n_0^2-1\right)}{k_0 n_0^2} v\frac{\partial}{\partial w}, \tag{8b}$$

$$\hat{Z}^{t(\mathrm{II})} = 0. \tag{8c}$$

The angular and spatial shifts can be obtained by substituting the related operators and effective Jones matrix into Eq. (6) and solving the integrals. For the fundamental Gaussian incident pulse, the calculation yields (see more details in Appendixes C and D)

$$\left\langle k_{X^a,y,Z^a}^a \right\rangle_0^{a,0} = \left\langle k_{X^a,y,Z^a}^{a(\mathrm{I})} \right\rangle_0^{a,0} + \left\langle k_{X^a,y,Z^a}^{a(\mathrm{II})} \right\rangle_0^{a,0}, \tag{9a}$$

$$\left\langle k_{X^a}^{a(\mathrm{I})} \right\rangle_0^{a,0} = \frac{\gamma^a}{2D}\frac{\partial \ln Q^{a2}}{\partial\theta_0}, \tag{9b}$$

$$\left\langle k_{Z^a}^{a(\mathrm{I})} \right\rangle_0^{a,0} = n_0^a k_0, \tag{9c}$$

$$\left\langle k_y^{a(\mathrm{I})} \right\rangle_0^{a,0} = \frac{\mathrm{Re}\left(e^{X^i *} e^y\right)\left[\left(f_p^a\right)^2 Y_p^a - \left(f_s^a\right)^2 Y_s^a\right]}{D} Q^{a2}, \tag{9d}$$

$$\left\langle k_{X^t}^{t(\mathrm{II})} \right\rangle_0^{t,0} = \left(\frac{1}{\cos^2\theta_0}+2\right)\frac{1-n_0^2}{4n_0 D}\tan\theta_0^t, \tag{9e}$$

$$\left\langle k_{Z^t}^{t(\mathrm{II})} \right\rangle_0^{t,0} = \left(\frac{1}{\cos^2\theta_0}+2\right)\frac{n_0^2-1}{4n_0 D}, \tag{9f}$$

$$\left\langle y^{a(\mathrm{I})} \right\rangle_0^{t,0} = -k_0\frac{\mathrm{Im}\left(e^{X^i *} e^y\right)\left[\left(f_p^a\right)^2 Y_p^a + \left(f_s^a\right)^2 Y_s^a\right]}{Q^{a2}}. \tag{9g}$$

Here the shifts have been decomposed into two parts: the first-order terms (I) and the second-order terms (II), in which $f_{p,s}^{r,t}$ is the Fresnel coefficients of the central wave vector (subscripts p and s denotes the components parallel and perpendicular to incident plane, respectively), $Q^{a2} = |f_p^a e^{X^i}|^2 + |f_s^a e^{y}|^2$, and $D = k_0 w_0^2/2$ is the Rayleigh length. Equations (9b) and (9e) represent the first- and second-order angular GH shifts, respectively, whereas Eqs. (9c) and (9f) represent the first- and second-order longitudinal wave-vector shifts, respectively. Particularly, Eqs. (9d) and (9g) give the angular and spatial IF shifts, which do not have the second-order terms. Change of the fundamental Gaussian pulse orientation keeps the shifts invariant due to its rotational symmetry. As we can see, the first-order terms depends on the polarization, as were also reported in Refs. [18,22], while the second-order terms of the angular shifts are still of the same order of D^{-1}, independent of polarization. Also, we can see the relation between the second-order terms in Eqs. (9e) and (9f),

$$\cos\theta_0^t \langle k_{X^t}^{t(\mathrm{II})}\rangle_0^{t,0} + \sin\theta_0^t \langle k_{Z^t}^{t(\mathrm{II})}\rangle_0^{t,0} = 0. \tag{10}$$

For spatial shifts, the nonzero term is the IF shift of refraction due to the partial refraction and reflection. The longitudinal spatial shift also is absent because the chromatic dispersion is omitted.

When the higher vortex structure is introduced into the pulse, the pulse will acquire additional shifts that depend on both the orientation and topological charge l. The calculation yields the first-order terms of angular shifts (see Appendix C),

$$\langle k_{X^a}^{a(\mathrm{I})}\rangle_{\Theta,\Phi}^{a} = \langle k_{X^a}^{a(\mathrm{I})}\rangle_0^{a,0} + |l|\Big[(1-\sin^2\Theta\cos^2\Phi)\langle k_{X^a}^{a(\mathrm{I})}\rangle_0^{a,0} - \frac{\gamma^a \sin^2\Theta \sin 2\Phi}{2}\langle k_y^{a(\mathrm{I})}\rangle_0^{a,0}\Big], \tag{11a}$$

$$\langle k_y^{a(\mathrm{I})}\rangle_{\Theta,\Phi}^{a} = \langle k_y^{a(\mathrm{I})}\rangle_0^{a,0} + |l|\Big[(1-\sin^2\Theta\sin^2\Phi)\langle k_y^{a(\mathrm{I})}\rangle_0^{a,0} - \frac{\sin^2\Theta \sin 2\Phi}{2\gamma^a}\langle k_{X^a}^{a(\mathrm{I})}\rangle_0^{a,0}\Big], \tag{11b}$$

$$\langle k_{Z^a}^{a(\mathrm{I})}\rangle_{\Theta,\Phi}^{a} = \langle k_{Z^a}^{a(\mathrm{I})}\rangle_0^{a,0} - |l|\Big[\frac{n_0^a \sin 2\Theta\cos\Phi}{2\gamma^a}\langle k_{X^a}^{a(\mathrm{I})}\rangle_0^{a,0} + \frac{n_0^a \sin 2\Theta\cos\Phi}{2}\langle k_y^{a(\mathrm{I})}\rangle_0^{a,0}\Big], \tag{11c}$$

and the second-order terms,

$$\langle k_{X^t}^{a(\mathrm{II})}\rangle_{\Theta,\Phi}^{t} = \frac{(1-n_0^2)}{4n_0 D}\tan\theta_0^t\Big[(|l|+1)\Big(\frac{1}{\cos^2\theta_0}+1\Big) - |l|\sin^2\Theta\Big(\frac{\cos^2\Phi}{\cos^2\theta_0}+\sin^2\Phi\Big)+1\Big], \tag{12a}$$

$$\langle k_{Z^t}^{a(\mathrm{II})}\rangle_{\Theta,\Phi}^{t} = \frac{(n_0^2-1)}{4n_0 D}\Big[(|l|+1)\Big(\frac{1}{\cos^2\theta_0}+1\Big) - |l|\sin^2\Theta\Big(\frac{\cos^2\Phi}{\cos^2\theta_0}+\sin^2\Phi\Big)+1\Big]. \tag{12b}$$

We can see from Eqs. (11a)–(11c), the shifts of wave vector are linearly dependent on $|l|$. In addition, the second and third terms on the right-hand side of Eqs. (11a)–(11c) demonstrate self-coupling and cross-coupling behaviors, respectively. They are tunable by adjusting the orientation angle, Θ and Φ. When the angles, Θ and Φ, are both chosen as $\pi/2$ (or $\pi/2$ and 0), the first-order terms reduce to the results of type A (or type B) reported in Ref. [22], except for the cross-coupling terms. When our 3D model degenerates into the two-dimensional (2D) model in Ref. [22], the cross-coupling terms disappears due to the infinite Rayleigh length along the corresponding direction, leading to the complete agreement of our present results with those presented in Ref. [22]. The cross-coupling between two transversal components and longitudinal component also give rise to the shifts in $k_{Z^a}^{a(\mathrm{I})}$. For the case of the vortex with longitudinal orientation (i.e., $\Theta = 0$ and $\Phi = 0$), all the cross-coupling terms just disappeared, where the first-order terms are the same as those for the monochromatic beam [16]. It is suggested that we can choose some specific Θ and Φ to maximize (or minimize) the sensitivity of these shifts to the OAM, as discussed in the next section. Besides, the additional second-order terms in Eqs. (12a) and (12b) have the same relationship as Eq. (10).

Meanwhile, we can derive the first-order terms of spatial shifts for a tilted vortex pulse as (see Appendix D),

$$\langle X^{a(\mathrm{I})}\rangle_{\Theta,\Phi}^{a} = l\frac{w_0^2}{2\gamma^a}\cos\Theta\langle k_y^a\rangle_0^{a,0}, \tag{13a}$$

$$\langle y^{a(\mathrm{I})}\rangle_{\Theta,\Phi}^{a} = \langle y^a\rangle_0^{a,0} - l\frac{\gamma^a w_0^2}{2}\cos\Theta\langle k_X^{a(\mathrm{I})}\rangle_0^{a,0}, \tag{13b}$$

$$\langle Z^a\rangle_{\Theta,\Phi}^{a} = l\frac{w_0^2}{2n_0^a\gamma^a}\sin\Theta\sin\Phi\langle k_X^{a(\mathrm{I})}\rangle_0^{a,0} - l\frac{w_0^2}{2n_0^a}\sin\Theta\cos\Phi\langle k_y^a\rangle_0^{a,0}, \tag{13c}$$

which represent the spatial GH shifts, IF shifts, and longitudinal shifts, respectively. At the same time, we have the second-order terms (see also Appendix D)

$$\langle X^{t(\mathrm{II})}\rangle_{\Theta,\Phi}^{a} = -\frac{l\sin\Theta\sin\Phi(n_0^2-1)}{2k_0\gamma^t\cos^2\theta_0 n_0^2}, \tag{14a}$$

$$\langle y^{t(\mathrm{II})}\rangle_{\Theta,\Phi}^{a} = l\frac{\cos\Theta\tan\theta_0(n_0^2-1)}{2k_0 n_0^2} + l\frac{\sin\Theta\cos\Phi(n_0^2-1)}{2k_0 n_0^2}, \tag{14b}$$

which rely on l linearly. The independence on spatial waists or duration time of pulse suggests the robustness of spatial shifts. Another most striking feature is that the angular shifts can be exchanged to the spatial shifts through the vortex structure [17]. For some specific Θ and Φ, Eqs. (13) and (14) reduce to the results reported in Refs. [16,22]. Interestingly, the first-order terms were interpreted as the real spatial shifts induced from imaginary angular shifts [18], while the remaining terms including $\langle y^a\rangle_0^a$ and second-order terms are related to the spin Hall effect and OAM Hall effect, respectively.

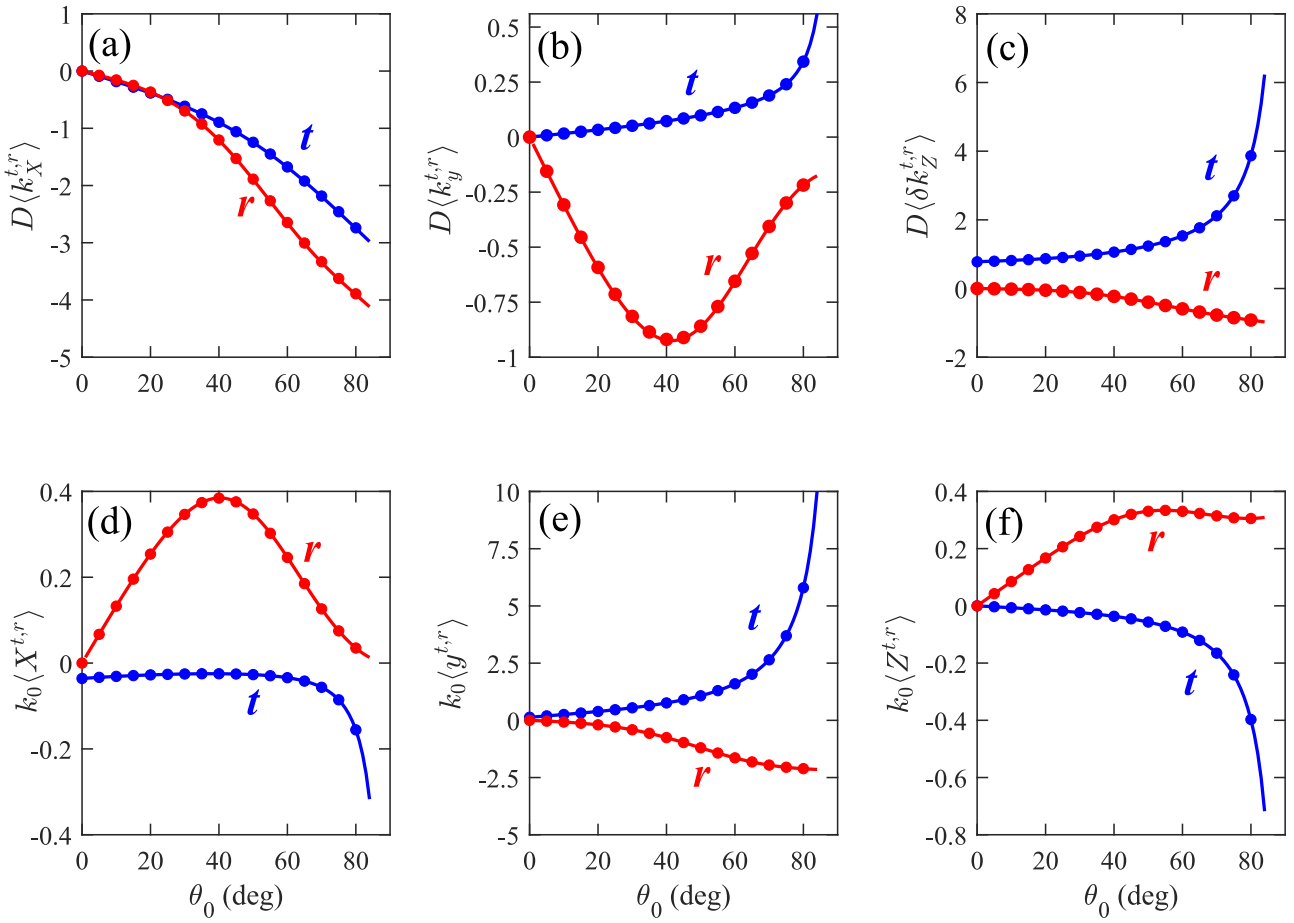

FIG. 2. Analytical results (curves) and numerical results (symbols) for angular and spatial shifts of the refracted (t) and reflected (r) STVPs with a topological charge $l = 1$ and an orientation of $\Theta = \pi/3$ and $\Phi = \pi/6$, as a function of the incidence angle θ_0. Several parameters are chosen as follows: the refractive index of the medium $n_0 = 1.5$, wavelength $\lambda = 632$ nm, waist $w_0 = 201$ μm, and transversal polarization $\mathbf{e}_\perp = [(1+i)\mathbf{e}_{X^i} + \mathbf{e}_y]/\sqrt{3}$.

In the derivation of the above analytical expressions, two approximations have been made: a second-order approximation for the correlation between the incident and refracted or reflected wave vectors (see Appendix A), and a first-order approximation for the Fresnel field transformation matrix (see Appendix B). To confirm the accuracy of these derived analytical expressions, we have conducted precise numerical simulations of these shifts without these approximations by directly utilizing Eqs. (A2) and (B2). We display in Fig. 2 the curves of the spatial and angular shifts as the incident angle is changed. As can be seen from the figure, the magnitudes of spatial shifts (first column) and angular shifts (second column) are at the orders of D^{-1} and k^{-1}, respectively. As the incident angle increases from 0 to 90 degrees, most of these shifts also increment from nearly zero to their maximum values. However, there are some exceptions. For instance, the angular shift k_y^r of the reflected pulse reaches a maximum near the Brewster angle [14], which also results in an enhancement when it is cross-coupled to spatial shifts X^r or Z^r, as shown in Figs. 2(d) or 2(f). The longitudinal angular shift δk_Z^r is not zero even when the incident angle is zero, mainly contributed by the second-order terms, as can be seen from Eqs. (9e) and (12b).

III. INFLUENCE OF THE ORIENTATION OF VORTICES ON THE SHIFTS

There is a more intuitive way to show spatial and angular shifts given by Eqs. (11a)–(14b). As shown in Appendix C, the expectation values of u, v, and w have a simpler relationship with their expectation values for the fundamental Gaussian pulse,

$$\begin{pmatrix} \langle u\rangle^a_{\Theta,\Phi} - \langle u\rangle^a_0 \\ \langle v\rangle^a_{\Theta,\Phi} - \langle u\rangle^a_0 \\ \langle w\rangle^a_{\Theta,\Phi} - \langle u\rangle^a_0 \end{pmatrix} = |l|\tilde{T}(\Theta,\Phi)\begin{pmatrix} \langle u\rangle^a_0 \\ \langle v\rangle^a_0 \\ \langle w\rangle^a_0 \end{pmatrix}, \quad (15)$$

where

$$\tilde{T}(\Theta,\Phi) = R^\dagger(\Theta,\Phi)\begin{pmatrix} 1 & 0 & 0 \\ 0 & 1 & 0 \\ 0 & 0 & 0 \end{pmatrix}R(\Theta,\Phi),$$

$\langle u, v\rangle^a_0 \neq 0$, and $\langle w\rangle^a_0 = 0$. In wave-vector space, we can define a constant fundamental vector $\tilde{\mathbf{U}}^a_0 = \langle u\rangle^a_0\mathbf{e}_{X^a} + \langle v\rangle^a_0\mathbf{e}_{y^a} + \langle w\rangle^a_0\mathbf{e}_{Z^a}$, which can also be represented in the form $\tilde{\mathbf{U}}^a_0 = \langle u'\rangle^a_0\mathbf{e}_{X'^a} + \langle v'\rangle^a_0\mathbf{e}_{y^a} + \langle w'\rangle^a_0\mathbf{e}_{Z'^a}$ in the frame (X'^a, y'^a, Z'^a) aligned with the vortex line of the incident pulse [i.e., $(\mathbf{e}_{X^a}, \mathbf{e}_{y^a}, \mathbf{e}_{Z^a}) = (\mathbf{e}_{X'^a}, \mathbf{e}_{y^a}, \mathbf{e}_{Z'^a})R(\Theta,\Phi)$]. The

components can be obtained from the original one by $(\langle u'\rangle_0^a, \langle v'\rangle_0^a, \langle w'\rangle_0^a)^T = R(\Theta, \Phi)(\langle u\rangle_0^a, \langle v\rangle_0^a, \langle w\rangle_0^a)^T$. We can also define the vector $\mathbf{U}_{\Theta,\Phi}^a$ for the titled high-order vortex pulse in a similar way. Then, Eq. (15) can be further written as

$$\langle u'\rangle_{\Theta,\Phi}^a = (|l|+1)\langle u'\rangle_0^a, \tag{16a}$$

$$\langle v'\rangle_{\Theta,\Phi}^a = (|l|+1)\langle v'\rangle_0^a, \tag{16b}$$

$$\langle w'\rangle_{\Theta,\Phi}^a = \langle w'\rangle_0^a. \tag{16c}$$

The above equations indicate that the high-order components parallel to vortex plane are $|l|+1$ times the fundamental components, while the component parallel to vortex line remains unchanged. We can write $\mathbf{U}_{\Theta,\Phi}^a$ as

$$\tilde{\mathbf{U}}_{\Theta,\Phi}^a = \tilde{\mathbf{U}}_0^a + |l|\big[(\mathbf{e}_{X'^a}\cdot\tilde{\mathbf{U}}_0^a)\mathbf{e}_{X'^a} + (\mathbf{e}_{y'}\cdot\tilde{\mathbf{U}}_0^a)\mathbf{e}_{y'}\big]. \tag{17}$$

This relation, unaffected by the optical property of the medium and environmental configuration, is only dependent on the pulse structure including the spatial and polarized parts. Thus we refer to $\tilde{\mathbf{U}}_{\Theta,\Phi}^a$ as the *isotropic angular-shift vector*. It can be regarded as a natural extension of the coupling relationship of the longitudinally orientated case [18]. According to Eq. (4), the angular shifts are just equal to the product of $k_0\mathbf{U}_{\Theta,\Phi}^a$ and

$$\hat{\mathbf{F}}^a = \begin{pmatrix} \gamma^a & 0 & 0 \\ 0 & 1 & 0 \\ 0 & 0 & n_0^a \end{pmatrix}, \tag{18}$$

which describes the environmental configuration including the incidence angle and the refractive index of the material. By substituting Eqs. (17) and (18) into Eq. (4), we obtain the relations of the first-order angular shifts between the high-order and fundamental cases,

$$\begin{aligned} D\Delta\mathbf{k}_{\Theta,\Phi}^{a(\mathrm{I})} = {} & D\Delta\mathbf{k}_0^a + |l|\big[(\mathbf{e}_{X'^a}^a)^T D\Delta\mathbf{k}_0^a\big]\tilde{\mathbf{e}}_{X'^a}^a \\ & + |l|\big[(\mathbf{e}_{y'^a}^a)^T D\Delta\mathbf{k}_0^a\big]\tilde{\mathbf{e}}_{y'^a}^a, \end{aligned} \tag{19}$$

where the vector $\Delta\mathbf{k}_{\Theta,\Phi}^{a(\mathrm{I})}$ is defined by $\langle k_{X^a}^{a(\mathrm{I})}\rangle_{\Theta,\Phi}^a\mathbf{e}_{X^a} + \langle k_y^{a(\mathrm{I})}\rangle_{\Theta,\Phi}^a\mathbf{e}_y + \langle \delta k_{Z^a}^{a(\mathrm{I})}\rangle\mathbf{e}_{Z^a}$, being scaled by D^{-1}. Here $\tilde{\mathbf{e}}_{X'^a,y'^a}^a$ and $\mathbf{e}_{X'^a,y'^a}^a$ are the vectors on the vortex plane of pulse in wave-vector space (i.e., $\tilde{\mathbf{e}}_{X'^a,y'^a}^a = \hat{\mathbf{F}}^a\mathbf{e}_{X'^a,y'^a}$) and in spatial space [i.e., $\mathbf{e}_{X'^a,y'^a}^a = (\hat{\mathbf{F}}^a)^{-1}\mathbf{e}_{X'^a,y'^a}$], respectively. In fact, the basis $(\tilde{\mathbf{e}}_{X'^a}^a, \tilde{\mathbf{e}}_{y'^a}^a, \tilde{\mathbf{e}}_{Z'^a}^a)$ is the dual basis of $(\mathbf{e}_{X'^a}^a, \mathbf{e}_{y'^a}^a, \mathbf{e}_{Z'^a}^a)$. Both of them are nonorthogonal bases due to deformation. The last two terms on the right-hand side of Eq. (19), parallel to the vortex plane, are actually the tangent components of $\Delta\mathbf{k}_0^a$ based on parallelogram decomposition, characterizing the angular-angular coupling.

The above procedure can also be employed to analyze the spatial shifts. The expectation values of $i\partial_u$, $i\partial_v$, and $i\partial_w$ have the following relationship:

$$\begin{pmatrix} \langle i\partial_u\rangle_{\Theta,\Phi}^a - \langle i\partial_u\rangle_0^{a,0} \\ \langle i\partial_v\rangle_{\Theta,\Phi}^a - \langle i\partial_v\rangle_0^{a,0} \\ \langle i\partial_w\rangle_{\Theta,\Phi}^a - \langle i\partial_w\rangle_0^{a,0} \end{pmatrix} = lT(\Theta,\Phi)\begin{pmatrix} \langle u\rangle_0^{a,0} \\ \langle v\rangle_0^{a,0} \\ \langle w\rangle_0^{a,0} \end{pmatrix}, \tag{20}$$

where

$$T(\Theta,\Phi) = k_0 DR^\dagger(\Theta,\Phi)\begin{pmatrix} 0 & 1 & 0 \\ -1 & 0 & 0 \\ 0 & 0 & 0 \end{pmatrix}R(\Theta,\Phi).$$

We can also refer to $\mathbf{U}_{\Theta,\Phi}^a = \langle i\partial_u\rangle_{\Theta,\Phi}^a\mathbf{e}_{X^a} + \langle i\partial_v\rangle_{\Theta,\Phi}^a\mathbf{e}_{y^a} + \langle i\partial_w\rangle_{\Theta,\Phi}^a\mathbf{e}_{Z^a}$ as the *isotropic spatial-shift vector*. Then, the spatial-shift vector $\Delta\mathbf{r}_{\Theta,\Phi}^a$ equals $k_0^{-1}(\hat{\mathbf{F}}^a)^{-1}\tilde{\mathbf{U}}_{\Theta,\Phi}^a$. For the components of the frame (X'^a, y', Z'^a), Eq. (20) can be further simplified as

$$\langle i\partial_{u'}\rangle_{\Theta,\Phi}^a = \langle i\partial_{u'}\rangle_0^a + lk_0 D\langle v'\rangle_0^a, \tag{21a}$$

$$\langle i\partial_{v'}\rangle_{\Theta,\Phi}^a = \langle i\partial_{v'}\rangle_0^a - lk_0 D\langle v'\rangle_0^a, \tag{21b}$$

$$\langle i\partial_{w'}\rangle_{\Theta,\Phi}^a = \langle i\partial_{w'}\rangle_0^a. \tag{21c}$$

Eventually, we obtain the relation for spatial shifts,

$$\begin{aligned} k_0\Delta\mathbf{r}_{\Theta,\Phi}^{a(\mathrm{I})} = {} & k_0\Delta\mathbf{r}_0^a + l\big[(\mathbf{e}_{y'^a}^a)^T D\Delta\mathbf{k}_0^a\big]\mathbf{e}_{X'^a}^a \\ & - l\big[(\mathbf{e}_{X'^a}^a)^T D\Delta\mathbf{k}_0^a\big]\mathbf{e}_{y'^a}^a, \end{aligned} \tag{22}$$

where the vector $\Delta\mathbf{r}_{\Theta,\Phi}^{a(\mathrm{I})}$ is defined by $\langle X^{a(\mathrm{I})}\rangle_{\Theta,\Phi}^a\mathbf{e}_{X^a} + \langle y^{a(\mathrm{I})}\rangle_{\Theta,\Phi}^a\mathbf{e}_y + \langle Z^{a(\mathrm{I})}\rangle_{\Theta,\Phi}^a\mathbf{e}_{Z^a}$, being scaled by k_0^{-1}. Distinguishing from the angular-angular coupling, angular-spatial coupling features the rule of projection decomposition and cross-correlation between the X'^a and y'^a direction, as indicated in the last two terms on the right-hand side of Eq. (22).

The above coupling mechanisms have also been vividly depicted in Fig. 3. We have identified every orientation as an intersection point of the direction vector and an ellipsoid, where the ellipsoid is the same as the isointensity surface of the fundamental Gaussian pulse. The point is also employed as the starting point of the shift vector. In this way, these ellipsoids actually represent the parameter spaces of orientation, and the shift vector field on them can be seen as a function of this parameter space. The isotropic envelope of the fundamental pulse is deformed from a sphere to an ellipsoid after refraction with the emergence of unified angular shift, as shown in Fig. 3(a). The ellipsoid and shift vector field on it can be simultaneously deformed backed to a sphere and a fundamental *isotropic angular-shift vector field* by $(\hat{\mathbf{F}}^a)^{-1}$, as shown in Fig. 3(d). Increasing the topological charge by one induces an additional *isotropic angular-shift vector field*, which is actually spherical tangent components of the fundamental vector field, as shown in Fig. 3(e). It can further be deformed into the induced angular-vector field that is also a tangent vector field of the ellipsoid by $\hat{\mathbf{F}}^a$. Given the orientation of the vortex line, we can obtain the corresponding tangent vector. Specifically, the field have two zero points, as shown in Fig. 3(b), almost along the X^t axis. Therefore, the shift vector of the pulse with the vortex line oriented along this direction will not be changed by increasing the topological charge. Meanwhile, by rotating this induced *isotropic angular-shift vector field* 90 degree clockwise along the oriented axis, we can obtain the induced *isotropic spatial-shift vector field*, as shown in Fig. 3(f), which can be deformed by $(\hat{\mathbf{F}}^a)^{-1}$ into the induced spatial-vector field, as shown in Fig. 3(c). These shift vector fields induced by increasing topological charges have two singularities; although they have a Poincaré index of $+1$, the angular-shift vector field is of a source-sink type, whereas

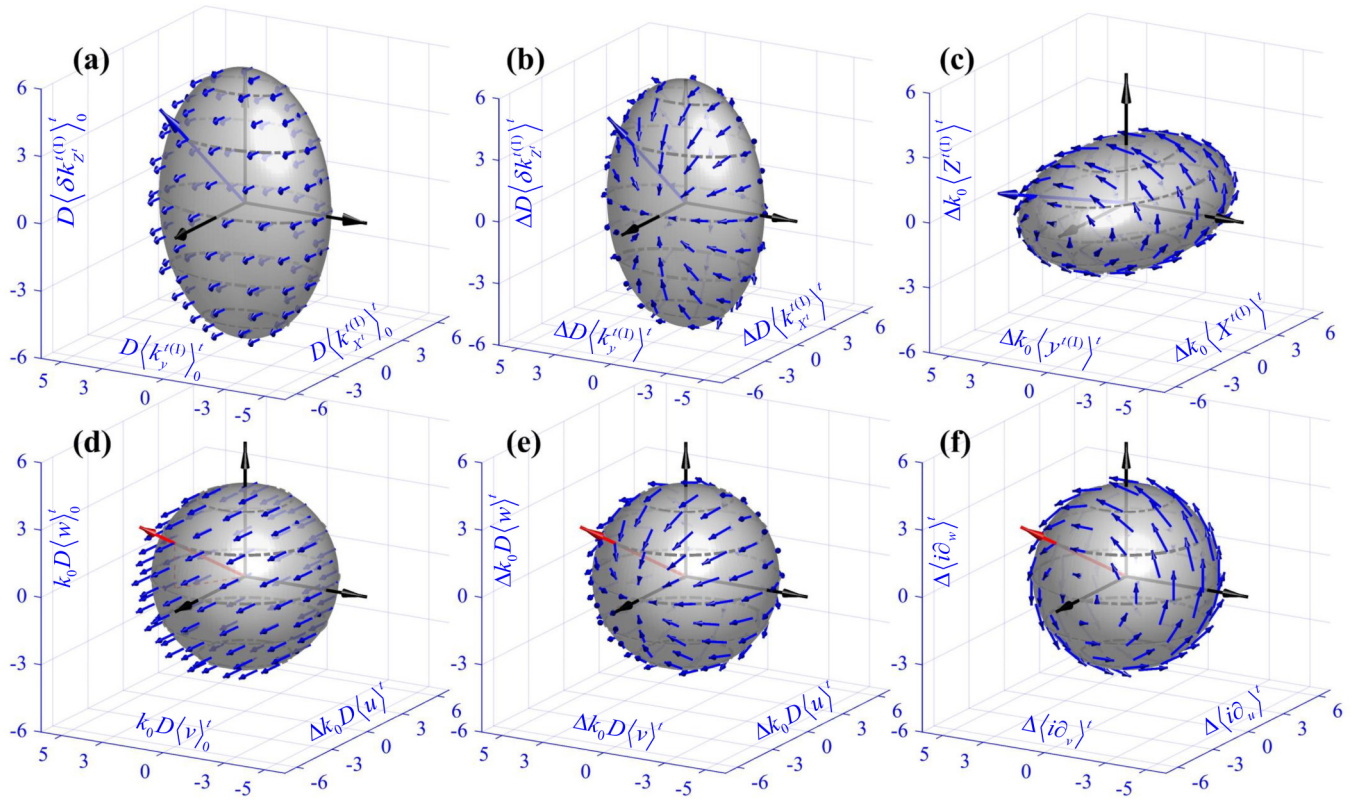

FIG. 3. The shift vectors related to the refracted pulse as a function of the orientation of vortex line. Each orientation corresponds to an intersection point of the orientation vector and the ellipsoid. The point is also chosen as the starting point of the shift vector. Specifically, the ellipsoids in panels (a) and (b) represent the isointensity surfaces of the refracted fundamental Gaussian pulse in wave-vector space, while panel (c) shows the surface in spatial space. The sphere in panels (d), (e) and (f) is predeformed, representing the incident fundamental Gaussian pulse's isointensity surfaces. In every subplot, the scales serve to measure the magnitude of the shift vectors. The first-order angular-shift vectors of the fundamental pulse (a) can induce angular-shift vectors (b) and spatial-shift vectors (c) by increasing one topological charge. Three ellipsoids and three shift-vector fields can be simultaneously deformed by the tensor $\hat{\mathbf{F}}^a$ into three spheres with (d) the fundamental *isotropic angular-shift vector field*, (e) the induced *isotropic angular-vector field*, and (f) the *isotropic spatial-shift vector field*, respectively. The incident angle is 60 degrees and other parameters are the same as those in Fig. 2

the spatial-shift vector field is of a circulation type. These singularities also exhibit robustness to deformations of the parameter space.

IV. CONSERVATION LAWS OF TRANSVERSAL LINEAR MOMENTUM AND VERTICAL ANGULAR MOMENTUM

The translational symmetry of configuration along the x and y directions implies that transversal momentum of the pulse must be conserved on reflection and refraction,

$$Q^{r2}\langle k_{x,y}\rangle^r_{\Theta,\Phi} + n_0\frac{\cos\theta_0^t}{\cos\theta_0}Q^{t2}\langle k_{x,y}\rangle^t_{\Theta,\Phi} = \langle k_{x,y}\rangle^i_{\Theta,\Phi}. \quad (23)$$

Here we assume that medium is nonmagnetic, $\mu = 1$. The above equation gives constraints on the components in the laboratory coordinate frame (x, y, z), as shown in Fig. 1(a). For the fundamental Gaussian pulse, our results given in Eq. (9a) includes the two additional terms of second-order angular shifts compared with previous results, which had been proven to satisfy the above conservation laws [18]. They contribute additional transversal linear momentum,

$$\langle k_x^{(\mathrm{II})}\rangle_0^{t,0} = \cos\theta_0^t\langle k_{X^t}^{t(\mathrm{II})}\rangle_0^{t,0} + \sin\theta_0^t\langle k_{Z^t}^{t(\mathrm{II})}\rangle_0^{t,0}. \quad (24)$$

Note that the above equation is just equivalent to zero according to Eq. (10). Therefore, the fundamental shifts satisfy the conversation laws. For angular shifts of the tilted STVP, we can prove that every first-order terms in Eqs. (11) satisfies the conservation law: (I) Self-coupling parts for the reflection and refraction are just equal to the corresponding shifts of fundamental Gaussian pulse times the same constant, thereby satisfies the conservation law. (II) For the cross-coupling parts, such as the last term of $\langle k^{a(\mathrm{I})}_{X^a,y^a}\rangle^a_{\Theta,\Phi}$ and the last two terms of $\langle k^{a(\mathrm{I})}_{Z^a}\rangle^a_{\Theta,\Phi}$ in Eqs. (11), we can substitute it into Eq. (23) to obtain the requirements of the conservation. The requirements are

$$-\cos^2\theta_0 Q^{r2}\langle k_y^{r(\mathrm{I})}\rangle_0^r\gamma^r + n_0\cos^2\theta_0^t Q^{t2}\langle k_y^{t(\mathrm{I})}\rangle_0^t\gamma^t = 0 \quad (25)$$

for the angular GH shifts $\langle k^{a(\mathrm{I})}_{X^a}\rangle^a_{\Theta,\Phi}$,

$$\cos\theta_0 Q^{r2}\langle k_{X^r}^{r(\mathrm{I})}\rangle_0^r\Big/\gamma^r + n_0\cos\theta_0^t Q^{t2}\langle k_{X^t}^{t(\mathrm{I})}\rangle_0^t\Big/\gamma^t = 0 \quad (26)$$

for the angular IF shifts $\langle k^{a(\mathrm{I})}_{y^a}\rangle^a_{\Theta,\Phi}$, and

$$\sin\theta_0\cos\theta_0 n_0 Q^{r2}\langle k_y^{r(\mathrm{I})}\rangle_0^r + \sin\theta_0^t\cos\theta_0^t n_0 Q^{t2}\langle k_y^{t(\mathrm{I})}\rangle_0^t = 0, \quad (27a)$$

$$\sin\theta_0\cos\theta_0 n_0 Q^{r2}\langle k_{X^r}^{r(\mathrm{I})}\rangle_0^r \Big/ \gamma^r + \sin\theta_0^t\cos\theta_0^t n_0 Q^{t2}\langle k_{X^t}^{t(\mathrm{I})}\rangle_0^t \Big/ \gamma^t = 0 \tag{27b}$$

for the longitudinal wave-vector shifts $\langle k_{Z^a}^{a(\mathrm{I})}\rangle_{\Theta,\Phi}^a$, respectively. By using $\gamma^r = -1$, $\gamma^t = \cos\theta_0/\cos\theta_0^t$, and $n_0 = \sin\theta_0/\sin\theta_0^t$, Eqs. (25)–(27) can be reduced to

$$-Q^{r2}\langle k_X^{r(\mathrm{I})}\rangle_0^r + n_0\frac{\cos^2\theta_0^t}{\cos^2\theta_0}Q^{t2}\langle k_X^{t(\mathrm{I})}\rangle_0^t = 0, \tag{28a}$$

$$Q^{r2}\langle k_y^{r(\mathrm{I})}\rangle_0^r + n_0\frac{\cos\theta_0^t}{\cos\theta_0}Q^{t2}\langle k_y^{t(\mathrm{I})}\rangle_0^t = 0, \tag{28b}$$

which just returns to the conservation laws for the first-order shift of a fundamental Gaussian pulse along the x and y directions. Besides, the second-order terms given in Eqs. (12) contribute zeros to $\langle k_x^{(\mathrm{II})}\rangle_{\Theta,\Phi}^t$ based on Eq. (10). These terms thereby also satisfy the conversion law. Therefore, total angular shifts of the tilted STVP satisfy the conversation law of transversal linear momentum.

In addition to linear momentum conservation, the rotational symmetry along the z axis gives the conservation equation for z components of total angular momentum,

$$Q^{r2}\langle J_z\rangle_{\Theta,\Phi}^r + n_0\frac{\cos\theta_0^t}{\cos\theta_0}Q^{t2}\langle J_z\rangle_{\Theta,\Phi}^t = \langle J_z\rangle_{\Theta,\Phi}^i, \tag{29}$$

where total AM consists of spin AM, intrinsic OAM, and extrinsic OAM: $\mathbf{J}^a = \mathbf{S}^a + \mathbf{L}^{ai} + \mathbf{L}^{ae}$. Specifically, the unified polarization determines spin AM $\mathbf{S}^a = 2\mathrm{Im}(e^{X^{a*}}e^{y^a})\mathbf{e}_{Z^a}$, whereas the spatial shift along the y direction determines extrinsic OAM $\mathbf{L}^{ae} = k_0\langle y^a\rangle\mathbf{e}_{X^a}$. For the fundamental Gaussian pulse without intrinsic OAM, the spatial shift $\langle y^{a(\mathrm{I})}\rangle_0^{t,0}$ given in Eq. (9a) is the same as the result in Ref. [18] satisfying conservation law of AM.

For higher-order titled STVPs, we should consider the intrinsic OAM. However, there is a controversy about the intrinsic OAM of STVPs: one claim is that the circularly symmetric STVPs with topological charge l carries $l\hbar/2$ of intrinsic OAM per photon in free space [28–30], whereas the other claim is that this value is $l\hbar$ under the same condition [31,32]. Here we calculate the intrinsic OAM based on the second claim. Although the profile of the pulse at refraction is deformed and cannot be described by standard or elliptic LG modes, as shown in Fig. 1(e), we can still calculate its intrinsic OAM. In fact, the operator of the intrinsic OAM of STVPs can be written as $\mathbf{L}^{ai} = i\nabla^a \times \mathbf{k}^a$ in the second claim. By substituting it into Eq. (6) and calculating the integral, we can obtain expectation of the components of intrinsic OAM:

$$\langle L_{X^a}^{ai}\rangle_{\Theta,\Phi}^a = \left(n_0^a + 1/n_0^a\right)l\sin\Theta\cos\Phi/2, \tag{30a}$$

$$\langle L_{y^a}^{ai}\rangle_{\Theta,\Phi}^a = \left(\gamma^a/n_0^a + n_0^a/\gamma^a\right)l\sin\Theta\sin\Phi/2, \tag{30b}$$

$$\langle L_{Z^a}^{ai}\rangle_{\Theta,\Phi}^a = (\gamma^a + 1/\gamma^a)l\cos\Theta/2. \tag{30c}$$

The above equation indicates that the orientation of intrinsic OAM, affected by the deformation of pulse, is neither along the vortex line at incidence nor along the vortex line at reflection or refraction. Eventually, z components of total AM at incidence, reflection, and refraction can be written as

$$\langle J_z\rangle_{\Theta,\Phi}^a = \cos\theta_0^a\langle S_{Z^a}\rangle_{\Theta,\Phi}^a - \sin\theta_0^a\langle L_{X^a}^{ai}\rangle_{\Theta,\Phi}^a + \cos\theta_0^a\langle L_{Z^a}^{ai}\rangle_{\Theta,\Phi}^a - k_0\sin\theta_0^a\langle y^a\rangle_{\Theta,\Phi}^a. \tag{31}$$

By combining Eqs. (13), (14), (28), (30), and (31), we can prove that they indeed satisfy the conversation law given by Eq. (29). The confirmation of the conversation law suggests the rationality of the intrinsic OAM we used. Reverse reasoning from Eq. (29) suggests a method for calculating $\langle y^a\rangle_{\Theta,\Phi}^a$. It should be noted that the result obtained by using this method excludes the cross-coupling term $\cos\Theta\langle k_X^{a(\mathrm{I})}\rangle_0^{a,0}l\gamma^a w_0^2/2$, which does not conflict with Eq. (29) because of its compatibility with the equation of linear momentum conservation law.

V. CONCLUSION

Under the approximation of second-order wave vector connection and first-order Fresnel coefficients, an analytic derivation for the spatial and angular shifts of a 3D STVP with an arbitrarily oriented OAM at planar reflection and refraction has been presented. These results are in excellent agreement with the precise numerical calculations and at the same time extend the studies of longitudinal and transversal vortices in Refs. [16,22] to a more general situation. These results highlight the fact that the influence of orientation, to some extent, can be regarded as an isotropic problem after distinguishing a deformation tensor. It is found that the angular shifts and spatial shifts induced by the topological charge number can be described by two tangent vector fields on the sphere, respectively. Moreover, conservation laws of linear and angular momentum have also been examined, especially emphasizing the importance of the intrinsic OAM. Our study is expected to not only guide a possible solution on recent controversy on the intrinsic OAM of STVP [28–32] but also provide theoretical support for precise manipulation on the STVPs. Another further investigation can include chromatic dispersion to study the Winger time delay.

ACKNOWLEDGMENTS

This work was supported by the National Natural Science Foundation of China (12034016, 61975169), the National Key R&D Program of China (2023YFA1407200), the Natural Science Foundation of Fujian Province of China (2021J02002), and the program for New Century Excellent Talents in University of China (NCET-13-0495).

APPENDIX A: WAVE VECTOR AND POSITION OPERATORS AT REFRACTION

For the wave vector of the incident pulse, the transformation between the components of laboratory coordinate frame and accompanying coordinate frame is

$$\begin{aligned} k_x^i &= \cos\theta_0 k_{X^i} + \sin\theta_0 k_{Z^i}, \\ k_z^i &= -\sin\theta_0 k_{X^i} + \cos\theta_0 k_{Z^i}, \\ k_y^i &= k_y. \end{aligned} \tag{A1}$$

Snell's law gives the relationship between the incident wave vector and the refracted wave vector as follows:

$$k_{x,y}^t = k_{x,y}^i,$$
$$k_z^t = \sqrt{n_0^2\left[\left(k_x^i\right)^2 + \left(k_y^i\right)^2 + \left(k_z^i\right)^2\right] - \left(k_x^i\right)^2 - \left(k_y^i\right)^2}, \quad \text{(A2)}$$

where we have ignored the frequency dependence of the refractive index $n(\omega) \approx n_0$. Similarly, the transformations between the components for the refracted pulse are

$$k_{X^t}^t = \cos\theta_0^t k_x^t - \sin\theta_0^t k_z^t, \quad k_{Z^t}^t = \sin\theta_0^t k_x^t + \cos\theta_0^t k_z^t. \quad \text{(A3)}$$

Here, k_y remains unchanged and will be omitted hereafter. By combining Eqs. (A1) and (A2), we can represent Eq. (A3) as a functions of the variables,

$$u_1 = k_{X^i}/k_0, \quad u_2 = k_y/k_0, \quad u_3 = k_{Z^i}/k_0 - 1, \quad \text{(A4)}$$

which shows that

$$k_{X^t}^t = k_0\cos\theta_0^t[u_1\cos\theta_0 + (u_3+1)\sin\theta_0] - k_0\sin\theta_0^t\sqrt{n_0^2\left[u_1^2+u_2^2+(u_3+1)^2\right] - [u_1\cos\theta_0 + (u_3+1)\sin\theta_0]^2 - u_2^2},$$
$$k_{Z^t}^t = k_0\sin\theta_0^t[u_1\cos\theta_0 + (u_3+1)\sin\theta_0] + k_0\cos\theta_0^t\sqrt{n_0^2\left[u_1^2+u_2^2+(u_3+1)^2\right] - [u_1\cos\theta_0 + (u_3+1)\sin\theta_0]^2 - u_2^2}. \quad \text{(A5)}$$

Performing a Taylor expansion of the above equation, we can obtain the first two-order terms,

$$k_{X^t}^t \approx \sum_{i=1}^{3}\frac{\partial k_{X^t}^t}{\partial u_i}\bigg|_0 u_i + \sum_{i,j=1}^{3}\frac{\partial^2 k_{X^t}^t}{\partial u_i\partial u_j}\bigg|_0 u_i u_j = \gamma^t k_0 u_1 - \frac{k_0\tan\theta_0^t\left(n_0^2-1\right)}{2n_0}\left(\frac{u_1^2}{\cos^2\theta_0^t} + u_2^2\right),$$
$$\delta k_{Z^t}^t \approx \sum_{i=1}^{3}\frac{\partial k_{Z^t}^t}{\partial u_i}\bigg|_0 u_i + \sum_{i,j=1}^{3}\frac{\partial^2 k_{Z^t}^t}{\partial u_i\partial u_j}\bigg|_0 u_i u_j = n_0 k_0 u_3 + \frac{k_0\left(n_0^2-1\right)}{2n_0}\left(\frac{u_1^2}{\cos^2\theta_0^t} + u_2^2\right), \quad \text{(A6)}$$

where $\delta k_{Z^t}^t = k_{Z^t}^t - n_0 k_0$. By substituting Eqs. (A4) into Eqs. (A6), we obtain the connection of wave vectors in a second-order approximation.

The position operators at refraction can also be expended in the basis $(i\partial/\partial u_1, i\partial/\partial u_2, i\partial/\partial u_3)$, that is,

$$\hat{X}^t, y, Z^t = i\frac{\partial}{\partial k_{X^t,y,Z^t}^t} = \sum_{i=1}^{3}\frac{\partial u_i}{\partial k_{X^t,y,Z^t}^t} i\frac{\partial}{\partial u_i}. \quad \text{(A7)}$$

Note that the expectation of $i\partial_{u_i}$ for a Gaussian pulse is the same order as that of u_i. Therefore, the second-order approximation of the position operators for a Gaussian pulse involves the zero- and first-order terms of the Jacobian matrix

$$\frac{\partial(u_1,u_2,u_3)}{\partial\left(k_{X^t}^t, k_y^t, k_{Z^t}^t\right)},$$

which can be further determined by calculating the inverse matrix of the Jacobian matrix

$$\frac{\partial\left(k_{X^t}^t, k_y^t, k_{Z^t}^t\right)}{\partial(u_1,u_2,u_3)}.$$

From Eqs. (A6), it yields

$$\frac{\partial\left(k_{X^t}^t, k_y^t, k_{Z^t}^t\right)}{\partial(u_1,u_2,u_3)} = k_0\begin{pmatrix} \gamma^t - \frac{\tan\theta_0^t\left(n_0^2-1\right)}{n_0\cos^2\theta_0}u_1 & 0 & \frac{\left(n_0^2-1\right)}{n_0\cos^2\theta_0}u_2 \\ -\frac{\tan\theta_0^t\left(n_0^2-1\right)}{n_0}u_1 & 1 & \frac{\left(n_0^2-1\right)}{n_0}u_2 \\ 0 & 0 & n_0 \end{pmatrix}. \quad \text{(A8)}$$

After inverting Eq. (A8) under zero- and first-order approximations and some algebraic calculations, we have

$$\frac{\partial(u_1,u_2,u_3)}{\partial\left(k_{X^t}^t, k_y^t, k_{Z^t}^t\right)} = \frac{1}{k_0}\begin{pmatrix} \frac{1}{\gamma^t} & 0 & -\frac{\sec^2\theta_0}{\gamma^t}\left(1-\frac{1}{n_0^2}\right)u_1 \\ \frac{\tan\theta_0^t}{\gamma^t}\left(n_0-\frac{1}{n_0}\right)u_2 & 1 & -\left(1-\frac{1}{n_0^2}\right)u_2 \\ 0 & 0 & \frac{1}{n_0} \end{pmatrix}. \quad \text{(A9)}$$

By substituting Eq. (A9) into Eq. (A7) and denoting (u_1, u_2, u_3) as (u, v, w), we eventually obtain the second-order approximation of the position operators,

$$\hat{X}^t = i\frac{1}{k_0\gamma^t}\frac{\partial}{\partial u} - i\frac{\left(n_0^2-1\right)}{k_0\gamma^t n_0^2\cos^2\theta_0}u\frac{\partial}{\partial w}, \quad \hat{y}^t = i\frac{1}{k_0}\frac{\partial}{\partial v} + i\frac{\tan\theta_0\left(n_0^2-1\right)}{k_0 n_0^2}v\frac{\partial}{\partial u} - i\frac{\left(n_0^2-1\right)}{k_0 n_0^2}v\frac{\partial}{\partial w}, \quad \hat{Z}^t = i\frac{1}{k_0 n_0}\frac{\partial}{\partial w}. \quad \text{(A10)}$$

APPENDIX B: EFFECTIVE JONES MATRIX

In this Appendix, we summarize the method presented in Ref. [18] to calculate the transformation between the incident and the refracted or reflected monochromatic 2D field under a first-order approximation of the Fresnel formula. Here, we present its 3D version for the polychromatic pulse. The Fresnel formula can be written as follows:

$$\begin{aligned}\left(\tilde{E}^a_\theta(\mathbf{k}^a), \tilde{E}^a_\varphi(\mathbf{k}^a), 0\right)^T &= \mathbf{F}^a(\mathbf{k}^i)\left(\tilde{E}^i_\theta(\mathbf{k}^i), \tilde{E}^i_\varphi(\mathbf{k}^i), 0\right)^T,\\ \mathbf{F}^a(\mathbf{k}^i) &= \begin{pmatrix} f^a_p(\mathbf{k}^i) & 0 & 0\\ 0 & f^a_s(\mathbf{k}^i) & 0\\ 0 & 0 & 1\end{pmatrix},\end{aligned} \tag{B1}$$

where p mode $\tilde{E}^a_\theta(\mathbf{k}^a)$ and s mode $\tilde{E}^a_\varphi(\mathbf{k}^a)$ are the polar and azimuthal component of field $\tilde{\mathbf{E}}^a$ of the wave vector $\mathbf{k}^a$ in the spherical coordinate frame. Fresnel coefficients $f^a_{p,s}$ depend on $\mathbf{k}^i$ (actually on the polar angle θ^i and frequency ω of $\mathbf{k}^i$) in the following way [1]:

$$\begin{aligned} f^t_p(\mathbf{k}^i) &= \frac{2\cos\theta^i(\mathbf{k}^i)}{n(\mathbf{k}^i)\cos\theta^i(\mathbf{k}^i)+\cos\theta^t(\mathbf{k}^i)},\\ f^t_s(\mathbf{k}^i) &= \frac{2\cos\theta^i(\mathbf{k}^i)}{\cos\theta^i(\mathbf{k}^i)+n(\mathbf{k}^i)\cos\theta^t(\mathbf{k}^i)},\\ f^r_p(\mathbf{k}^i) &= \frac{n(\mathbf{k}^i)\cos\theta^i(\mathbf{k}^i)-\cos\theta^t(\mathbf{k}^i)}{n(\mathbf{k}^i)\cos\theta^i(\mathbf{k}^i)+\cos\theta^t(\mathbf{k}^i)},\\ f^r_s(\mathbf{k}^i) &= \frac{\cos\theta^i(\mathbf{k}^i)-n(\mathbf{k}^i)\cos\theta^t(\mathbf{k}^i)}{\cos\theta^i(\mathbf{k}^i)+n(\mathbf{k}^i)\cos\theta^t(\mathbf{k}^i)},\end{aligned} \tag{B2}$$

where the refraction angle as the functions of wave vectors can be expressed as $\theta^t(\mathbf{k}^i) = \arcsin[n^{-1}(\mathbf{k}^i)\sin\theta^i(\mathbf{k}^i)]$. The transformation between the components of spherical coordinate and accompanying coordinate is

$$\left[\tilde{E}^a_\theta(\mathbf{k}^a), \tilde{E}^a_\varphi(\mathbf{k}^a), 0\right]^T = U(\mathbf{k}^a)\left[\tilde{E}^a_{X^a}(\mathbf{k}^a), \tilde{E}^a_y(\mathbf{k}^a), \tilde{E}^a_{Z^a}(\mathbf{k}^a)\right]^T, \tag{B3}$$

where the matrix $U(\mathbf{k}^a)$ is defined by

$$U(\mathbf{k}^a) = R_y\left[\theta^a_0(\mathbf{k}^i)\right]R_z[\varphi^a(\mathbf{k}^i)]R^\dagger_y[\theta_0(\mathbf{k}^i)], \tag{B4}$$

with R_y and R_z representing the rotation matrix along the y and z axes. By combining Eqs. (B1) and (B3), we can obtain the field transformation between the incident and the refracted or reflected pulse,

$$\begin{aligned}&\left[\tilde{E}^a_{X^a}(\mathbf{k}^a), \tilde{E}^a_y(\mathbf{k}^a), \tilde{E}^a_{Z^a}(\mathbf{k}^a)\right]^T\\ &\quad= \mathbf{T}^a(\mathbf{k}^a)\left[\tilde{E}^i_{Z^i}(\mathbf{k}^i), \tilde{E}^i_y(\mathbf{k}^i), \tilde{E}^i_{Z^i}(\mathbf{k}^i)\right]^T,\end{aligned} \tag{B5}$$

where the effective Jones matrix $\mathbf{T}^a(\mathbf{k}^a) = U^\dagger(\mathbf{k}^a)\mathbf{F}^a(\mathbf{k}^i)U(\mathbf{k}^i)$. Considering the paraxial and quasimonochromatic approximation of the pulse, it is reasonable to consider the first-order terms of $\mathbf{T}^a(\mathbf{k}^a) = U^\dagger(\mathbf{k}^a)\mathbf{F}^a(\mathbf{k}^i)U(\mathbf{k}^i)$, which can be calculated as follows:

$$\begin{aligned}\mathbf{F}^a = \mathrm{diag}\Bigg[&f^a_p\left(1+u\frac{\partial\ln f^a_p}{\partial\theta}+wm_0\frac{\partial\ln f^a_p}{\partial n_0}\right),\\ &f^a_s\left(1++u\frac{\partial\ln f^a_s}{\partial\theta}+wm_0\frac{\partial\ln f^a_s}{\partial n_0}\right), 1\Bigg].\end{aligned} \tag{B6}$$

Here $m_0 = \partial_\omega n|_{\omega_0} = n_0(1-v^0_p/v^0_g)$ describes the relative difference between group velocity and the group velocity at the central frequency. In this paper, we do not consider the terms $wm_0\partial\ln f^a_{p,s}/\partial n$. It is valid when that the group velocity of the medium equals its phase velocity, or when the chromatic dispersion at center frequency can be ignored. Eventually, the first-order approximation of the effective Jones matrix can be written as

$$\mathbf{T}^a(\mathbf{k}^a) \approx \mathbf{T}^a(u,v) = \mathbf{T}^{a0} + u\mathbf{T}^{au} + v\mathbf{T}^{av}, \tag{B7}$$

where

$$\begin{aligned}\mathbf{T}^{a0} &= \begin{bmatrix} f^a_p & 0\\ 0 & f^a_s\end{bmatrix}, \quad \mathbf{T}^{au} = \begin{bmatrix} f^a_p X^a_p & 0\\ 0 & f^a_s X^a_s\end{bmatrix},\\ \mathbf{T}^{av} &= \begin{bmatrix} 0 & f^a_p Y^a_p\\ -f^a_s Y^a_s & 0\end{bmatrix},\end{aligned} \tag{B8}$$

and $\mathbf{T}^{aw} = 0$. Here $X^a_{p,s} = \partial_\theta\ln f^a_{p,s}|_{\theta_0}$, $Y^a_{p,s} = [1 - f^a_{s,p}/(\gamma^a f^a_{p,s})]\cot\theta_0$, and the 3×3 matrices have been degenerated into 2×2 matrices by considering the negligibility of the Z^a components in the paraxial approximation.

Before applying the aforementioned field transformation formulas, we should acquire a more detailed understanding of the shifts we are calculating: Since the energy density of the pulse at position $\mathbf{r}$ is $I(\mathbf{r}) \propto \varepsilon|\mathrm{E}(\mathbf{r})|^2$, then, similar to the formula for calculating the mass centroid, the formula for calculating the energy centroid of the refracted or reflected pulses in the wave vector representation is

$$\langle\mathbf{r}^a\rangle^a = \frac{\iiint[\tilde{\mathbf{E}}'^a(\mathbf{k}^a)]^\dagger(i\nabla^a)\tilde{\mathbf{E}}'^a(\mathbf{k}^a)d\mathbf{k}^a}{\iiint|\tilde{\mathbf{E}}'^a(\mathbf{k}^a)|^2 d\mathbf{k}^a}. \tag{B9}$$

Similarly, we can define the average wave vector $\langle\mathbf{k}^a\rangle^a$. These six components are exactly the six types of shifts mentioned in the main text. It is important to note that, as the pulse changes over time, the energy centroid will also change with time, although the mean of wave vector will not change. We define the moment the pulse just arrives at the interface as $t = 0$. It is not difficult to show that its energy centroid at the moment t_0 would be

$$\langle\mathbf{r}^a(t_0)\rangle^a = \langle\mathbf{r}^a(0)\rangle^a + v^0_g\mathbf{n}(\Delta\langle\mathbf{k}^a\rangle^a)t_0, \tag{B10}$$

where v^0_g is group velocity, $\langle\mathbf{r}^a(0)\rangle^a$ is the spatial shift vector at $t = 0$, $\mathbf{n}(\mathbf{v})$ is the unit vector of $\mathbf{v}$, and $\Delta\langle\mathbf{k}^a\rangle^a = \langle\mathbf{k}^a\rangle^a - \mathbf{k}^a_0$ indicates the deviation of the mean of wave vector relative to the central wave vector. Therefore, as the pulse propagates, the orientation of $\Delta\langle\mathbf{k}^a\rangle^a$ can be transformed into spatial shift vector, which also explains why we refer to $\Delta\langle\mathbf{k}^a\rangle^a$ as the angular shift vector in the main text. We have also illustrated this process in Fig. 1(a).

It should be noted that the refracted field obtained in Eq. (B1) is just the amplitude of a plane wave with wave vector $\mathbf{k}$ but is not the representation of the refracted pulse in wave-vector space due to the inhomogeneity of distribution of refracted wave vectors. In fact, the representation of the refracted pulse is actually formulated as $\tilde{\mathbf{E}}'^a(\mathbf{k}^a) = [\partial(\mathbf{k}^i)/\partial(\mathbf{k}^a)]^{1/2}\tilde{\mathbf{E}}^a(\mathbf{k}^a)$. Therefore, by replacing the parameters from the refracted or reflected wave vectors $\mathbf{k}^a$ to the

incident wave vector $\mathbf{k}^i$, Eq. (B9) can be rewritten as

$$\langle O^a\rangle^a = \frac{\iiint [\tilde{\mathbf{E}}''^a(\mathbf{k}^i)]^\dagger \hat{O}^a(\mathbf{k}^i)\tilde{\mathbf{E}}''^a(\mathbf{k}^i)d\mathbf{k}^i}{\iiint |\tilde{\mathbf{E}}''^a(\mathbf{k}^i)|^2 d\mathbf{k}^i}. \tag{B11}$$

Here, O^a is the spatial or wave vector operator as a function of $\mathbf{k}^i$, as provided in Appendix A, and the field $\tilde{\mathbf{E}}''^a$ is the specific functional form of Eq. (B1) depending on $\mathbf{k}^i$. We can rewrite Eq. (B9) as

$$\tilde{\mathbf{E}}''^a(\mathbf{k}^i) = \tilde{\mathbf{E}}^a(\mathbf{k}^a) = \mathbf{F}^a(\mathbf{k}^i)\tilde{\mathbf{E}}^i(\mathbf{k}^i). \tag{B12}$$

By replacing the parameters from $\mathbf{k}^i$ to (u, v, w), we eventually obtain Eq. (6), which is consistence with that given in Refs. [5,18,22].

APPENDIX C: ANGULAR SHIFTS

The denominator in right-hand side of Eq. (B9) denoted Q^{a2} equals $|f_p^a e^{X^i}|^2 + f_s^a e^y|^2$ under the zeroth-order approximation and represents the intensity of refracted or reflected pulse. Based on Eq. (B9), the angular shifts of the tilted STVP with a vortex line along (Θ, Φ) have the form

$$\langle \Delta\mathbf{k}^a\rangle^a_{\Theta,\Phi} = \frac{1}{Q^{a2}}\iiint \Delta\mathbf{k}^a h(u, v)|\mathrm{LG}_l(u', v', w')|^2 du dv dw, \tag{C1}$$

with the new scaled components of the wave vector $(u', v', w')^T = R^\dagger(\Theta, \Phi)(u, v, w)^T$, LG mode $\mathrm{LG}_l(u', v', w') = \tilde{N}_l(u' + i\mathrm{sgn}(l)v')^{|l|}e^{-k_0^2 w_0^2(u'^2+v'^2+w'^2)/4}$, and polarization-dependent quadratic form

$$h(u, v) = \left(e^{X^i*}, e^{y*}\right)\mathbf{T}^T(u, v)\mathbf{T}(u, v)\left(e^{X^i}, e^y\right)^T. \tag{C2}$$

Equation (C2), given by Eq. (B7), can be linearly approximated as follows:

$$h(u, v) \approx h_0 + h_u u + h_v v + h_w w, \tag{C3}$$

where the expansion coefficients are

$$\begin{aligned} h_0 &= \left(e^{X^i*}, e^{y*}\right)(\mathbf{T}^{a0})^2\left(e^{X^i}, e^y\right)^T = Q^{a2}, \\ h_u &= \left(e^{X^i*}, e^{y*}\right)(\mathbf{T}^{auT}\mathbf{T}^{a0} + \mathbf{T}^{a0}\mathbf{T}^{au})\left(e^{X^i}, e^y\right)^T \\ &= \partial_\theta Q^{a2}, \\ h_v &= \left(e^{X^i*}, e^{y*}\right)(\mathbf{T}^{avT}\mathbf{T}^{a0} + \mathbf{T}^{a0}\mathbf{T}^{av})\left(e^{X^i}, e^y\right)^T \\ &= 2\mathrm{Re}\left(e^{X^i*}e^y\right)\left[\left(f_p^a\right)^2 Y_p^a - \left(f_s^a\right)^2 Y_s^a\right], \\ h_w &= 0. \end{aligned} \tag{C4}$$

To solve the integral in Eq. (C1), we represent all involving terms on the parameters (u', v', w'). First, the quadratic form is expended in the new scaled components, that is, $h(u, v) = h_0 + h_{u'}u' + h_{v'}v' + h_{w'}w'$. The relationship between these new expansion coefficients and the coefficients given in Eq. (C4) can be expressed as

$$(h_{u'}, h_{v'}, h_{w'})^T = R(\Theta, \Phi)(h_u, h_v, h_w)^T. \tag{C5}$$

Second, according to Eq. (4a), the first-order wave vector $\Delta\mathbf{k}^{a(\mathrm{I})}_{\Theta,\Phi}$ can represented as

$$\begin{aligned} \Delta\mathbf{k}^{a(\mathrm{I})} &= k_0\gamma^a u\mathbf{e}_{X^a} + k_0 v\mathbf{e}_y + k_0 n^a w\mathbf{e}_{Z^a} \\ &= k_0(\gamma^a\mathbf{e}_{X^a}, \mathbf{e}_y, n^a\mathbf{e}_{Z^a})R(\Theta, \Phi)(u', v', w')^T. \end{aligned} \tag{C6}$$

Third, the infinitesimal element is rewritten as $du'dv'dw' = dudvdw$. By substituting Eqs. (C5) and (C6) into Eq. (C1), and after some algebraic operations, we have

$$\begin{aligned} \langle \Delta\mathbf{k}^{a(\mathrm{I})}\rangle^a_{\Theta,\Phi} &= \frac{k_0}{Q^{a2}}(\gamma^a\mathbf{e}_{X^a}, \mathbf{e}_y, n^a\mathbf{e}_{Z^a})\begin{pmatrix} U \\ V \\ W \end{pmatrix}, \\ \begin{pmatrix} U \\ V \\ W \end{pmatrix} &= R^T(\Theta, \Phi)\begin{pmatrix} m_u^l & 0 & 0 \\ 0 & m_v^l & 0 \\ 0 & 0 & m_w^l \end{pmatrix} \\ &\quad \times R(\Theta, \Phi)\begin{pmatrix} h_u \\ h_v \\ h_w \end{pmatrix}. \end{aligned} \tag{C7}$$

Here m_u^l, m_v^l, and m_w^l are actually the second-order moments of LG modes, defined by

$$\begin{aligned} m_u^l &= \iiint u'^2|\mathrm{LG}_l(u', v', w')|^2 du dv dw \\ &= (|l| + 1)/(2k_0 D), \\ m_v^l &= \iiint v'^2|\mathrm{LG}_l(u', v', w')|^2 du dv dw \\ &= (|l| + 1)/(2k_0 D), \\ m_w^l &= \iiint w'^2|\mathrm{LG}_l(u', v', w')|^2 du dv dw \\ &= 1/(2k_0 D), \end{aligned} \tag{C8}$$

respectively. In above derivation, we have used some feature of LG modes, such as the odd-order moments equals zeros. Equation (C7) can also be explicitly represented as

$$\langle k_{X^a}^{a(\mathrm{I})}\rangle^a_{\Theta,\Phi} = \langle k_{X^a}^{a(\mathrm{I})}\rangle_0^{a,0} + |l|\left[(1 - \sin^2\Theta\cos^2\Phi)\langle k_{X^a}^{a(\mathrm{I})}\rangle_0^{a,0} - \frac{\gamma^a\sin^2\Theta\sin 2\Phi}{2}\langle k_y^{a(\mathrm{I})}\rangle_0^{a,0}\right], \tag{C9a}$$

$$\langle k_y^{a(\mathrm{I})}\rangle^a_{\Theta,\Phi} = \langle k_y^{a(\mathrm{I})}\rangle_0^{a,0} + |l|\left[(1 - \sin^2\Theta\sin^2\Phi)\langle k_y^{a(\mathrm{I})}\rangle_0^{a,0} - \frac{\sin^2\Theta\sin 2\Phi}{2\gamma^a}\langle k_{X^a}^{a(\mathrm{I})}\rangle_0^{a,0}\right], \tag{C9b}$$

$$\langle k_{Z^a}^{a(\mathrm{I})}\rangle^a_{\Theta,\Phi} = \langle k_{Z^a}^{a(\mathrm{I})}\rangle_0^{a,0} - |l|\left[\frac{n_0^a\sin 2\Theta\cos\Phi}{2\gamma^a}\langle k_{X^a}^{a(\mathrm{I})}\rangle_0^{a,0} + \frac{n_0^a\sin 2\Theta\cos\Phi}{2}\langle k_y^{a(\mathrm{I})}\rangle_0^{a,0}\right], \tag{C9c}$$

where $\langle k_X^{a(\mathrm{I})}\rangle_0^{a,0}$, $\langle k_y^{a(\mathrm{I})}\rangle_0^{a,0}$, and $\langle k_Z^{a(\mathrm{I})}\rangle_0^{a,0}$ are the angular shifts for the fundamental pulse with following forms:

$$\begin{aligned}\langle k_{X^a}^{a(\mathrm{I})}\rangle_0^{a,0} &= \gamma^a \frac{\partial_\theta \ln Q^{a2}}{2D},\\ \langle k_y^{a(\mathrm{I})}\rangle_0^{a,0} &= \mathrm{Re}\big(e^{X^{i*}} e^{y}\big)\frac{\big(f_p^a\big)^2 Y_p^a - (f_s^a)^2 Y_s^a}{DQ^{a2}},\\ \langle k_{Z^a}^{a(\mathrm{I})}\rangle_0^{a,0} &= 0. \end{aligned} \tag{C10}$$

In the above derivation, we have only considered the first-order wave vector $\Delta\mathbf{k}_{\Theta,\Phi}^{a(\mathrm{I})}$. Now, we intend to calculate the expectations of the second-order wave vector $\Delta\mathbf{k}_{\Theta,\Phi}^{a(\mathrm{II})}$ given in Eq. (5a). In the second-order approximation of the expectation, we only need consider the zeroth-order approximation of polarization-dependent quadratic form given in Eq. (C2). By exchanging the parameters (u, v, w) to (u', v', w'), this problem can also be attributed to calculate the second-order moment matrix of LG modes. Specifically, Eq. (C8) lists all nonzero elements of this matrix of LG modes. By utilizing $(u, v, w) = R(\Theta, \Phi)(u', v', w')$, it is straightforward to obtain

$$\begin{aligned}\langle u^2\rangle_{\Theta,\Phi}^a &= [|l|(1-\sin^2\Theta\cos^2\Phi)+1]/(2k_0D),\\ \langle v^2\rangle_{\Theta,\Phi}^a &= [|l|(1-\sin^2\Theta\sin^2\Phi)+1]/(2k_0D). \end{aligned} \tag{C11}$$

By substituting Eq. (C11) into Eq. (5a), we have

$$\begin{aligned}\big\langle k_{X^t}^{a(\mathrm{II})}\big\rangle_{\Theta,\Phi}^t &= \frac{\big(1-n_0^2\big)}{4n_0D}\tan\theta_0^t\Bigg[(|l|+1)\bigg(\frac{1}{\cos^2\theta_0}+1\bigg)\\ &\quad -|l|\sin^2\Theta\bigg(\frac{\cos^2\Phi}{\cos^2\theta_0}+\sin^2\Phi\bigg)+1\Bigg], \end{aligned} \tag{C12a}$$

$$\begin{aligned}\big\langle k_{Z^t}^{a(\mathrm{II})}\big\rangle_{\Theta,\Phi}^t &= \frac{\big(n_0^2-1\big)}{4n_0D}\Bigg[(|l|+1)\bigg(\frac{1}{\cos^2\theta_0}+1\bigg)\\ &\quad -|l|\sin^2\Theta\bigg(\frac{\cos^2\Phi}{\cos^2\theta_0}+\sin^2\Phi\bigg)+1\Bigg]. \end{aligned} \tag{C12b}$$

APPENDIX D: SPATIAL SHIFTS

The procedure of the derivation of spatial shifts is the same as the derivation of angular shifts but more complex. We first calculate the expectation of the first-order spatial shifts given in Eq. (A10). For a titled STVP, we also introduce new scaled components of spatial operator $(i\partial_{u'}, i\partial_{v'}, i\partial_{w'})$, which are connected with the original one by a rotational matrix,

$$(i\partial_u, i\partial_v, i\partial_w) = R(\Theta, \Phi)(i\partial_{u'}, i\partial_{v'}, i\partial_{w'}). \tag{D1}$$

The expectation of $i\partial_{u'}$, similar to Eq. (B9), can be calculated by

$$\begin{aligned}\langle i\partial_{u'}\rangle_{\Theta,\Phi}^a &= \frac{1}{Q^{a2}}\iiint \mathrm{LG}_l^*(u', v', w')\hat{P}_{u'}^a\\ &\quad\times \mathrm{LG}_l(u', v', w')du'dv'dw', \end{aligned} \tag{D2}$$

where $i\partial_{u'}$ and all of the related Jones matrices have been put in

$$\hat{P}_{u'}^a = \big(e^{X^{i*}}, e^{y*}\big)\mathbf{T}^{aT}(u, v)i\partial_{u'}\mathbf{T}^a(u, v)\big(e^{X^i}, e^{y}\big)^T. \tag{D3}$$

We can decompose $\hat{P}_{u'}^a$ into two parts, $\hat{P}_{u'}^{a(1)}$ and $\hat{P}_{u'}^{a(2)}$, defined as

$$\begin{aligned}\hat{P}_{u'}^{a(1)} &= i\big(e^{X^{i*}}, e^{y*}\big)\mathbf{T}^T(u, v)\mathbf{T}^{au'}\big(e^{X^i}, e^{y}\big)^T,\\ \hat{P}_{u'}^{a(2)} &= (h_0 + h_{u'}u' + h_{v'}v' + h_{w'}w')i\partial_{u'}, \end{aligned} \tag{D4}$$

where we have given the definition of h_0 and $h_{u'}$, etc. in Appendix C. Considering the odd-order moments of LG modes equal to zero, the expectation of $\hat{P}_{u'}^{a(1)}$ for the scalar LG modes can be resolved into

$$\begin{aligned}\big\langle\hat{P}_{u'}^{a(1)}\big\rangle_{\Theta,\Phi}^a &= i\big(e^{X^{i*}}, e^{y*}\big)\mathbf{T}^0\mathbf{T}^{au'}\big(e^{X^i}, e^{y}\big)^T/Q^{a2}\\ &= ih'_{u'}/Q^{a2}. \end{aligned} \tag{D5}$$

Here we denote $(e^{X^{i*}}, e^{y*})\mathbf{T}^0\mathbf{T}^{au'}(e^{X^i}, e^{y})^T$ as $h'_{u'}$. For the second part, we note that

$$\begin{aligned}\mathrm{LG}_l^* i\partial_{u'}\mathrm{LG}_l = {}& k_0D[\mathrm{sgn}(l)v'|\mathrm{LG}_{l-1}|^2\\ &+ iu'|\mathrm{LG}_{l-1}|^2 - iu'|\mathrm{LG}_l|^2]. \end{aligned} \tag{D6}$$

By combining Eqs. (D4) and (D6), we can resolve the expectation of $\hat{P}_{u'}^{a(2)}$ into following form:

$$\big\langle\hat{P}_{u'}^{a(2)}\big\rangle_{\Theta,\Phi}^a = \frac{k_0D}{Q^{a2}}\big[\mathrm{sgn}(l)h_{v'}m_v^{l-1} + ih_{u'}m_u^{l-1} - ih_{u'}m_u^l\big]. \tag{D7}$$

By combining Eqs. (D5), (D7), and (C8), we obtain

$$\langle i\partial_{u'}\rangle_{\Theta,\Phi}^a = [lh_{v'} + i(h'_{u'} - h_{u'}/2)]/Q^{a2}. \tag{D8}$$

The other two components, $i\partial_{v'}$ and $i\partial_{w'}$, can also be resolved in the same way. The calculated result shows

$$\begin{aligned}\langle i\partial_{v'}\rangle_{\Theta,\Phi}^a &= [-lh_{u'} + i(h'_{v'} - h_{v'}/2)]/Q^{a2},\\ \langle i\partial_{w'}\rangle_{\Theta,\Phi}^a &= i(h'_{w'} - h_{w'}/2)/Q^{a2}. \end{aligned} \tag{D9}$$

In analogy to $(h_{u'}, h_{v'}, h_{w'})$, $(h'_{u'}, h'_{v'}, h'_{w'})$ can be obtained by the rotation of the original one, namely,

$$(h'_{u'}, h'_{v'}, h'_{w'})^T = R(\Theta, \Phi)(h'_u, h'_v, h'_w)^T. \tag{D10}$$

It is not difficult to show that the original one satisfies

$$\begin{aligned}i(h'_u - h_u/2) &= 0,\\ i(h'_v - h_v/2) &= -\mathrm{Im}(e^{X_i*}e^y)\big[\big(f_p^a\big)^2Y_p^a + \big(f_s^a\big)^2Y_s^a\big],\\ i(h'_w - h_w/2) &= 0. \end{aligned} \tag{D11}$$

For the fundamental Gaussian pulse and the tilted angle $\Theta = 0$, $\Phi = 0$, we have

$$\begin{aligned}\langle i\partial_{u'}\rangle_0^{a,0} &= 0,\\ \langle i\partial_{v'}\rangle_0^{a,0} &= -\mathrm{Im}(e^{X_i*}e^y)\big[\big(f_p^a\big)^2Y_p^a + (f_s^a)^2Y_s^a\big]/Q^{a2},\\ \langle i\partial_{w'}\rangle_0^{a,0} &= 0. \end{aligned} \tag{D12}$$

Equation (D12) implies that only the IF shift $\langle\Delta y\rangle_0^{a,0} = -k_0\mathrm{Im}(e^{X_i*}e^y)[(f_p^a)^2Y_p^a + (f_s^a)^2Y_s^a]/Q^{a2}$ occurs. The reason is that our configuration is actually an example of partial reflection, while the GH shift only occurs at total reflection. When the topological charge increases along the orientation (Θ, Φ), we can combine Eqs. (C5), (D1), (D8)–(D10), and (D12) to

obtain the these scaled spatial shifts. The result shows

$$\begin{pmatrix} \langle i\partial_u\rangle^a_{\Theta,\Phi} - \langle i\partial_u\rangle^{a,0}_0 \\ \langle i\partial_v\rangle^a_{\Theta,\Phi} - \langle i\partial_v\rangle^{a,0}_0 \\ \langle i\partial_w\rangle^a_{\Theta,\Phi} - \langle i\partial_w\rangle^{a,0}_0 \end{pmatrix} = lT(\Theta,\Phi)\begin{pmatrix} \langle u\rangle^{a,0}_0 \\ \langle v\rangle^{a,0}_0 \\ \langle w\rangle^{a,0}_0 \end{pmatrix},$$

$$T(\Theta,\Phi) = k_0 DR^\dagger(\Theta,\Phi)\begin{pmatrix} 0 & 1 & 0 \\ -1 & 0 & 0 \\ 0 & 0 & 0 \end{pmatrix} \times R(\Theta,\Phi). \tag{D13}$$

Eventually, the expression of the first-order spatial shifts can be written as

$$\langle X^{a(\mathrm{I})}\rangle^a_{\Theta,\Phi} = l\frac{w_0^2}{2\gamma^a}\cos\Theta\langle k_y^a\rangle^{a,0}_0, \tag{D14a}$$

$$\langle y^{a(\mathrm{I})}\rangle^a_{\Theta,\Phi} = \langle y^a\rangle^{a,0}_0 - l\frac{\gamma^a w_0^2}{2}\cos\Theta\langle k_X^{a(\mathrm{I})}\rangle^{a,0}_0, \tag{D14b}$$

$$\langle Z^a\rangle^a_{\Theta,\Phi} = l\frac{w_0^2}{2n_0^a\gamma^a}\sin\Theta\sin\Phi\langle k_X^{a(\mathrm{I})}\rangle^{a,0}_0 - l\frac{w_0^2}{2n_0^a}\sin\Theta\cos\Phi\langle k_y^a\rangle^{a,0}_0, \tag{D14c}$$

Solving the second-order spatial shifts, as shown in Eq. (A10), can be attributed to solving the spatial-angular moment matrix of LG modes. The skill of derivation is the same as the previous section. Here we only provide the result. The new spatial-angular moment matrix is

$$\begin{pmatrix} \langle u'i\partial_{u'}\rangle^a_{\Theta,\Phi} & \langle u'i\partial_{v'}\rangle^a_{\Theta,\Phi} & \langle u'i\partial_{w'}\rangle^a_{\Theta,\Phi} \\ \langle v'i\partial_{u'}\rangle^a_{\Theta,\Phi} & \langle v'i\partial_{v'}\rangle^a_{\Theta,\Phi} & \langle v'i\partial_{w'}\rangle^a_{\Theta,\Phi} \\ \langle w'i\partial_{u'}\rangle^a_{\Theta,\Phi} & \langle w'i\partial_{v'}\rangle^a_{\Theta,\Phi} & \langle w'i\partial_{w'}\rangle^a_{\Theta,\Phi} \end{pmatrix} = \frac{1}{2}\begin{pmatrix} -i & -l & 0 \\ l & -i & 0 \\ 0 & 0 & -i \end{pmatrix}, \tag{D15}$$

which is independent on the polarization, frequency, and spatial waist of the pulse. After applying the rotation operator, the related elements of the original spatial-angular moment matrix take the form

$$\begin{aligned} \langle iu\partial_w\rangle^a_{\Theta,\Phi} &= l\sin\Theta\sin\Phi/2, \\ \langle iv\partial_u\rangle^a_{\Theta,\Phi} &= l\cos\Theta/2, \\ \langle iv\partial_w\rangle^a_{\Theta,\Phi} &= -l\sin\Theta\cos\Phi/2. \end{aligned} \tag{D16}$$

Specifically, the expression of orbital angular momentum presented in Eqs. (30) can be easily derived from above equation. By substituting Eq. (D16) into Eq. (A10), we can obtain the explicit expressions of the second-order spatial shifts (14).

[1] M. Born and E. Wolf, *Principles of Optics: Electromagnetic Theory of Propagation, Interference and Diffraction of Light*, 7th ed. (Cambridge University Press, 1999).

[2] F. Goos and H. Hänchen, Ein neuer und fundamentaler versuch zur totalreflexion, Ann. Phys. **436**, 333 (1947).

[3] K. Artmann, Berechnung der seitenversetzung des totalreflektierten strahles, Ann. Phys. **437**, 87 (1948).

[4] E. P. Wigner, Lower limit for the energy derivative of the scattering phase shift, Phys. Rev. **98**, 145 (1955).

[5] M. Mazanov and K. Y. Bliokh, Wigner time delays and Goos-Hänchen shifts of 2D quantum vortices scattered by potential barriers, J. Phys. A: Math. Theor. **55**, 404005 (2022).

[6] F. I. Fedorov, To the theory of total reflection, J. Opt. **15**, 14002 (2013).

[7] C. Imbert, Calculation and experimental proof of the transverse shift induced by total internal reflection of a circularly polarized light beam, Phys. Rev. D: Part. Fields **5**, 787 (1972).

[8] M. Onoda, S. Murakami, and N. Nagaosa, Hall effect of light, Phys. Rev. Lett. **93**, 083901 (2004).

[9] K. Y. Bliokh and Y. P. Bliokh, Conservation of angular momentum, transverse shift, and spin Hall effect in reflection and refraction of an electromagnetic wave packet, Phys. Rev. Lett. **96**, 073903 (2006).

[10] K. Y. Bliokh and Y. P. Bliokh, Polarization, transverse shifts, and angular momentum conservation laws in partial reflection and refraction of an electromagnetic wave packet, Phys. Rev. E **75**, 066609 (2007).

[11] O. Hosten and P. Kwiat, Observation of the spin Hall effect of light via weak measurements, Science **319**, 787 (2008).

[12] C. C. Chan and T. Tamir, Angular shift of a Gaussian beam reflected near the Brewster angle, Opt. Lett. **10**, 378 (1985).

[13] A. Aiello and J. P. Woerdman, Role of beam propagation in Goos–Hänchen and Imbert–Fedorov shifts, Opt. Lett. **33**, 1437 (2008).

[14] M. Merano, A. Aiello, M. Exter, and J. Woerdman, Observing angular deviations in specular reflection of light, Nat. Photon. **3**, 337 (2009).

[15] V. Fedoseyev, Spin-independent transverse shift of the centre of gravity of a reflected and of a refracted light beam, Opt. Commun. **193**, 9 (2001).

[16] K. Y. Bliokh, I. V. Shadrivov, and Y. S. Kivshar, Goos–Hänchen and Imbert–Fedorov shifts of polarized vortex beams, Opt. Lett. **34**, 389 (2009).

[17] M. Merano, N. Hermosa, J. P. Woerdman, and A. Aiello, How orbital angular momentum affects beam shifts in optical reflection, Phys. Rev. A **82**, 023817 (2010).

[18] K. Y. Bliokh and A. Aiello, Goos-Hänchen and Imbert-Fedorov beam shifts: An overview, J. Opt. **15**, 014001 (2013).

[19] N. Jhajj, I. Larkin, E. W. Rosenthal, S. Zahedpour, J. K. Wahlstrand, and H. M. Milchberg, Spatiotemporal optical vortices, Phys. Rev. X **6**, 031037 (2016).

[20] S. W. Hancock, S. Zahedpour, A. Goffin, and H. M. Milchberg, Free-space propagation of spatiotemporal optical vortices, Optica **6**, 1547 (2019).

[21] A. Chong, C. Wan, J. Chen, and Q. Zhan, Generation of spatiotemporal optical vortices with controllable transverse orbital angular momentum, Nat. Photon. **14**, 350 (2020).

[22] M. Mazanov, D. Sugic, M. A. Alonso, F. Nori, and K. Y. Bliokh, Transverse shifts and time delays of spatiotemporal vortex pulses reflected and refracted at a planar interface, Nanophotonics **11**, 737 (2022).

[23] H. Wang, C. Guo, W. Jin, A. Y. Song, and S. Fan, Engineering arbitrarily oriented spatiotemporal optical vortices using transmission nodal lines, Optica **8**, 966 (2021).

[24] Y. Zang, A. Mirando, and A. Chong, Spatiotemporal optical vortices with arbitrary orbital angular momentum orientation by astigmatic mode converters, Nanophotonics **11**, 745 (2022).

[25] J. Chen, L. Yu, C. Wan, and Q. Zhan, Spin-orbit coupling within tightly focused circularly polarized spatiotemporal vortex wavepacket, ACS Photonics **9**, 793 (2022).

[26] X. Meng, Y. Hu, C. Wan, and Q. Zhan, Optical vortex fields with an arbitrary orbital angular momentum orientation, Opt. Lett. **47**, 4568 (2022).

[27] M. A. Porras and S. W. Jolly, Control of vortex orientation of ultrashort optical pulses using a spatial chirp, Opt. Lett. **48**, 6448 (2023).

[28] S. W. Hancock, S. Zahedpour, and H. M. Milchberg, Mode structure and orbital angular momentum of spatiotemporal optical vortex pulses, Phys. Rev. Lett. **127**, 193901 (2021).

[29] M. A. Porras and S. W. Jolly, Transverse orbital angular momentum imparted upon focusing spatio-temporally coupled ultrashort pulses, arXiv:2309.01505 [Phys. Rev. A (to be published)].

[30] M. A. Porras, Transverse orbital angular momentum of spatiotemporal optical vortices, Prog. Electromagn. Res. **177**, 95 (2023).

[31] K. Y. Bliokh, Spatiotemporal vortex pulses: Angular momenta and spin-orbit interaction, Phys. Rev. Lett. **126**, 243601 (2021).

[32] K. Y. Bliokh, Orbital angular momentum of optical, acoustic, and quantum-mechanical spatiotemporal vortex pulses, Phys. Rev. A **107**, L031501 (2023).